CFLIT: Coexisting Federated Learning and Information Transfer

1

Zehong Lin, Graduate Student Member, IEEE, Hang Liu, Member, IEEE, and Ying-Jun Angela Zhang, Fellow, IEEE

Abstract

Future wireless networks are expected to support diverse mobile services, including artificial intelligence (AI) services and ubiquitous data transmissions, Federated learning (FL), as a revolutionary learning approach, enables collaborative AI model training across distributed mobile edge devices. By exploiting the superposition property of multiple-access channels, over-the-air computation allows concurrent model uploading from massive devices over the same radio resources, and thus significantly reduces the communication cost of FL. In this paper, we study the *coexistence* of over-the-air FL and traditional information transfer (IT) in a mobile edge network, where an access point (AP) coordinates a set of devices for over-the-air FL and serves multiple devices for information transfer in the meantime. We propose a coexisting federated learning and information transfer (CFLIT) communication framework, where the FL and IT devices share the wireless spectrum in an orthogonal frequency division multiplexing (OFDM) system. Under this framework, we aim to maximize the IT data rate and guarantee a given FL convergence performance by optimizing the long-term radio resource allocation. A key challenge that limits the spectrum efficiency of the coexisting system lies in the large overhead incurred by frequent communication between the server and edge devices for FL model aggregation. To address the challenge, we rigorously analyze the impact of the computation-to-communication ratio on the convergence of over-the-air FL in wireless fading channels. The analysis reveals the existence of an optimal computation-to-communication ratio that minimizes the amount of radio resources needed for over-the-air FL to converge to a given error tolerance. Based on the analysis, we propose a lowcomplexity online algorithm to jointly optimize the radio resource allocation for both the FL devices and IT devices. We further derive an analytical expression of the achievable data rate of IT users. Extensive numerical simulations verify the superior performance of the proposed design for the coexistence of FL and IT devices in wireless cellular systems.

Index Terms

Zehong Lin and Ying-Jun Angela Zhang are with the Department of Information Engineering, The Chinese University of Hong Kong, Hong Kong (e-mail: lz018@ie.cuhk.edu.hk; yjzhang@ie.cuhk.edu.hk). Hang Liu is with the Department of Electrical and Computer Engineering, National University of Singapore, Singapore 117583 (e-mail: hangliu@nus.edu.sg).

Edge intelligence, federated learning (FL), over-the-air computation, coexistence, orthogonal frequency-division multiplexing (OFDM), multiple access.

I. Introduction

The proliferation of mobile artificial intelligence (AI) services, such as autonomous driving and intelligent personal assistants, triggers the emergence of a new paradigm called *edge intelligence* [1]-[3], which migrates the training and inference processes of AI models from central cloud servers to the edge of wireless networks, i.e., edge servers and mobile devices. Federated learning (FL) [4] has been widely perceived as a promising edge learning framework that allows mobile devices to collaboratively train a shared AI model without disclosing the raw data. Specifically, mobile devices download the global model from an edge server, e.g., an access point (AP), for local model training and upload the updated local models to the edge server. The server then updates the global model by aggregating a linear combination of local models. To relieve the communication burden of FL model uploading and aggregation, over-the-air computation [5] has been introduced into the FL model aggregation process [6]. By exploiting the superposition property of multiple-access channels, over-the-air model aggregation allows massive devices to simultaneously transmit their local models using the same channel and coherently aligns the local models at the server. The required bandwidth and communication latency for overthe-air computation are independent of the number of devices, thus significantly reducing the communication cost for FL model aggregation.

Extensive studies have been conducted to design over-the-air FL systems in wireless networks [6]–[12]. Most prior work, however, considers over-the-air computation over narrow-band systems and is not applicable to modern broadband wireless networks. To facilitate broadband implementation, the recent work in [13] proposed a broadband over-the-air model aggregation approach in orthogonal frequency division multiplexing (OFDM) systems. Nonetheless, Ref. [13] ignored the coexistence of over-the-air FL with traditional information transfer (IT) services. Note that future wireless networks are required to support multiple devices with different data communication demands at the same time [14]–[16]. For instance, FL devices need to frequently communicate model information with the AP, which in the meanwhile serves another set of devices for data streaming. Therefore, it is of great importance to design a coexisting system to support the coexistence of over-the-air FL and IT in wireless networks. This motivates the work in this paper.

Designing the above coexisting system is a challenging task. Although over-the-air model aggregation greatly reduces the bandwidth cost compared with traditional FL, uploading high-dimensional model parameters to the edge server iteratively until model convergence still leads to an extremely high bandwidth cost. Such a high bandwidth consumption leaves very little spectrum for IT devices to transmit their data traffic. Therefore, minimizing the bandwidth consumption of over-the-air FL is a critical problem in the design of the coexisting system. Note that the total bandwidth consumption is sensitive to the total number of communication rounds, which is critically determined by the design of the over-the-air FL training process. Consequently, we shall carefully study the FL mechanism design to minimize the bandwidth consumption needed for convergence.

There are two main research directions towards minimizing the bandwidth consumption of FL in the literature: one is to reduce the communication bandwidth cost per communication round and the other is to reduce the total number of communication rounds for model update. On one hand, the communication cost in each round can be reduced by model compression [17]. Existing approaches for model compression are divided into two categories: quantization [18] and sparsification [19]. In the former, local models are quantized into finite-bit digits to reduce the amount of data in model uploading [20], [21]. In the latter, local gradients are transformed to low-dimensional vectors at the transmitters by exploiting the gradient sparsity and recovered at the server by compressed sensing [22]–[24]. On the other hand, the total number of communication rounds can be reduced by carefully selecting the computation-to-communication ratio. For example, [4], [25], [26] have reported that the number of model updates computed locally before uploading the local model parameters to the server for model aggregation critically determines the total number of communication rounds needed for convergence. Specifically, a smaller number of local updates (i.e., a lower computation-to-communication ratio) means more frequent model aggregation, and thus a higher communication cost. Meanwhile, a larger number of local updates (i.e., a higher computation-to-communication ratio) leads to infrequent model aggregation, which inevitably slows down the learning convergence especially when the data distribution across devices is heterogeneous. Inspired by this observation, the authors in [27] optimized the number of local updates to minimize the required number of FL communication rounds. Moreover, Refs. [28], [29] extended the result in [27] by taking the wireless network characteristics into account.

Although the current work in [22]–[24] has demonstrated the effectiveness of model compres-

sion on reducing the communication cost for over-the-air model aggregation, the number of model parameters after compression is still very large. For instance, the famous deep learning model AlexNet in [30] consists of more than 60 million parameters. Even the state-of-the-art gradient sparsification approach has compressed the transmitted local gradients with compression ratio of 10% [24], transmitting the sparisified model to the server still consumes a large amount of radio resources in each round. In light of this, reducing the required number of model communication rounds is critical to save the bandwidth cost. The prior work on the optimization of computation-to-communication ratio [27]–[29], however, considers conventional orthogonal transmission and is not applicable to over-the-air FL. For over-the-air FL, the wireless channel fading inevitably induces signal misalignment in model aggregation, which brings a considerable error in the aggregated global gradient. Such an error is coupled with the effect of local model updating during the training process and slows down the learning convergence rate [7]. Therefore, it is necessary to investigate the coupled impact of the model aggregation error and the number of local updates on the bandwidth consumption needed for the convergence of over-the-air FL. Nonetheless, this important study is largely overlooked in the literature.

In this paper, we study a coexisting federated learning and information transfer (CFLIT) system in a single-cell mobile edge network consisting of a single AP, a set of FL devices, and a set of IT devices. The AP coordinates the FL devices for over-the-air FL and simultaneously serves the IT devices for uplink IT using the same uplink spectrum. To minimize the bandwidth cost for FL, we first analyze the convergence behavior of over-the-air FL as a function of local model updates and the total number of communication rounds in a wireless fading channel. Based on the analysis, we optimize the key parameters, i.e., the number of local updates and the number of FL communication rounds, to minimize the radio resources needed for over-the-air model aggregation. Then, we formulate a radio resource allocation problem to simultaneously maximize the average IT data rate and guarantee the convergence of over-the-air FL in a given time horizon. The lack of non-causal information of future channel state makes it difficult to jointly optimize the long-term radio resource allocation for both the FL and IT devices with an offline scheme. To overcome this difficulty, we propose a low-complexity online algorithm to make real-time allocation decisions based on the current observation of channel state information (CSI). To the best of our knowledge, this is the first paper that studies the joint communication and learning design in a wireless network to support the coexistence of over-the-air FL and IT. The main contributions of this paper are summarized as follows.

- Bandwidth cost minimization for over-the-air FL: We theoretically analyze the achievable training loss of over-the-air FL under mild assumptions to characterize the impact of the computation-to-communication ratio on the over-the-air FL convergence. We then derive a closed-form expression of the optimal computation-to-communication ratio that yields the minimum number of communication rounds. The analysis provides a useful guideline on how to optimize the key parameters of FL for minimizing the bandwidth cost for over-the-air model aggregation.
- CFLIT communication framework: We develop a novel CFLIT communication framework to coordinate both over-the-air model aggregation and uplink data streaming. Specifically, the FL devices and the IT devices simultaneously transmit local model updates and general data streams, respectively, to the AP over time-varying broadband channels. We formulate a CFLIT radio resource allocation problem to maximize the average IT data rate and at the same time ensure FL convergence in a given duration. To minimize the radio resource consumption for FL convergence guarantee, the transceiver design and learning parameters are jointly taken into account.
- Low-complexity online algorithm for radio resource allocation: We propose an efficient threshold-based online subcarrier allocation algorithm for CFLIT by mimicking the offline optimal solution. Unlike the offline scheme, the proposed algorithm does not require the non-causal CSI of the entire time horizon. Instead, it relies on the instantaneous channel gains of IT devices in the current symbol duration only and allocates subcarriers based on an optimized threshold. Moreover, we provide theoretical performance analysis to prove the rate improvement of the proposed online algorithm.

Simulation results verify our theoretical analysis and show that the proposed online algorithm performs very close to the offline optimal solution. Moreover, the proposed design achieves a better FL performance and a higher average IT data rate compared with the baseline approaches.

The rest of this paper is organized as follows. In Section II, we describe the CFLIT system model and the problem formulation. In Section III, we present the convergence analysis for over-the-air FL. Based on this, we derive analytical expressions to optimize the number of local updates and the number of communication rounds. In Section IV, we propose an efficient online algorithm to optimize the subcarrier allocation and provide theoretical performance analysis. In Section V, we evaluate the proposed design via extensive simulations. Finally, we conclude the paper in Section VI.

Notations: We use regular letters, boldface lower-case letters, boldface upper-case letters, and calligraphy letters to denote scalars, vectors, matrices, and sets, respectively. The real and complex domains are denoted by \mathbb{R} and \mathbb{C} , respectively. We use $\mathcal{N}(\mu, \sigma^2)$ and $\mathcal{C}\mathcal{N}(\mu, \sigma^2)$ to denote the real and the circularly-symmetric complex Gaussian distributions with mean μ and variance σ^2 , respectively. We use x_i or x[i] to denote the i-th entry of vector \mathbf{x} , x_{ij} to denote the (i,j)-th entry of matrix \mathbf{X} , $|\mathcal{S}|$ to denote the cardinality of set \mathcal{S} , and $\mathbb{E}[\cdot]$ to denote the expectation operator.

II. SYSTEM MODEL AND PROBLEM FORMULATION

A. CFLIT System Model

We consider a single-cell CFLIT system, where K FL devices, indexed by $\mathcal{K}=\{1,\cdots,K\}$, collaboratively train an AI model by exchanging model information with an AP. At the same time, N IT devices, indexed by $\mathcal{N}=\{1,\cdots,N\}$, transmit information-bearing signals to the AP through the uplink channels. All the nodes are equipped with single antenna. As shown in [31], the uplink model uploading and aggregation incur a high bandwidth cost and act as the communication bottleneck of FL. To significantly reduce the communication cost for FL, we adopt the over-the-air computation technique to accelerate the uplink model aggregation. By employing OFDM modulation, the total uplink bandwidth is divided into M orthogonal OFDM subcarriers, indexed by $\mathcal{M}=\{1,\cdots,M\}$. The AP is in charge of allocating subcarriers to support the over-the-air model aggregation of the FL devices and the data transmissions from the IT devices. We consider a time horizon consisting of S OFDM symbols, which is sufficiently long for over-the-air FL to converge. The total number of available OFDM resource blocks (RBs) for accomplishing over-the-air FL and IT is MS. To avoid interference, each subcarrier is allocated to either over-the-air model aggregation or at most one IT device.

We assume a block fading channel model, where the channel coefficients between the devices and the AP evolve independently over each coherence block following the independent and identically distributed (i.i.d.) Gaussian distribution of $\mathcal{CN}(0,1)$. Suppose that the considered time interval of S OFDM symbols is much larger than the coherence block length. We need to consider long-term dynamic RB allocation over multiple blocks with varying channel coefficients. We consider a training-based channel estimation protocol where a number of time slots at the beginning of each coherence block is used to transmit pilots for uplink channel estimation. We ignore the overhead and error in channel estimation and assume that only the CSI of the current coherence block is available.

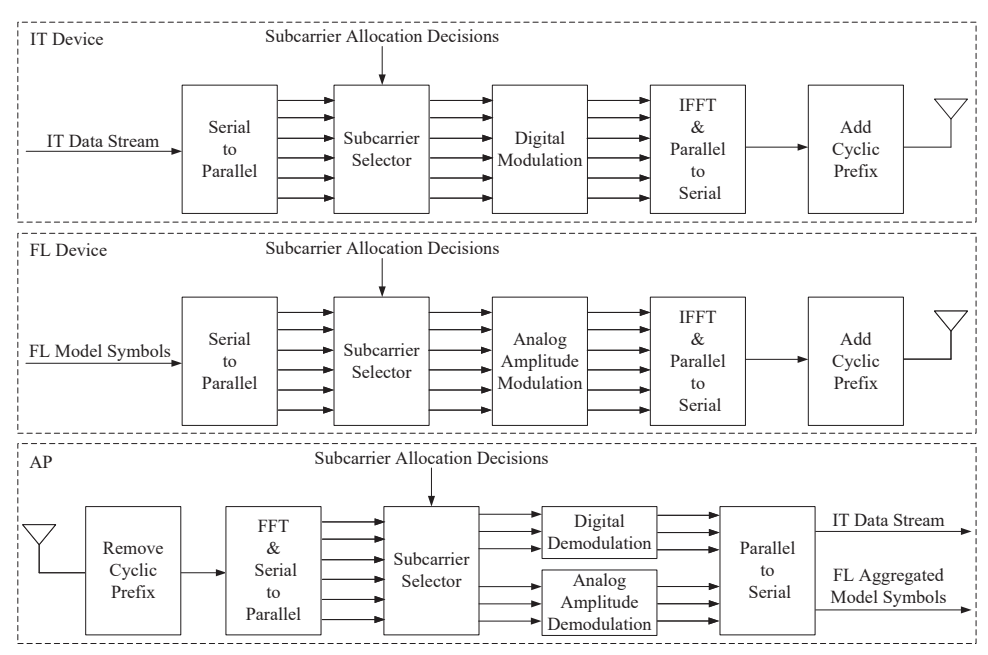


Fig. 1: The workflow of the transmitters and receiver.

The workflow of the transmitters and the receiver in the CFLIT system is shown in Fig. 1. On one hand, the data stream of each IT device is first segmented into parallel streams, which are then modulated into digital signals on the allocated subcarriers before being transmitted to the AP. On the other hand, the FL devices apply analog amplitude modulation to modulate the local model symbols into analog signals on the allocated subcarriers by a uniform waveform [13], e.g., a square wave. Then, the signals of all FL devices are amplified by their respective transmit scalars and transmitted simultaneously to the AP. The receiver of the AP performs digital demodulation on the subcarriers allocated to IT and performs analog amplitude demodulation on the other subcarriers. As a result, the AP is able to extract the data streams and over-the-air aggregated model symbols from the subcarriers accordingly.

Define $o_{m,s}$ as the binary subcarrier allocation indicator for over-the-air FL on the m-th subcarrier of the s-th OFDM symbol. We have $o_{m,s}=1$ if the m-th subcarrier of the s-th OFDM symbol is allocated to over-the-air model aggregation and $o_{m,s}=0$ otherwise. Moreover, we define $b_{n,m,s}$ as the binary subcarrier allocation indicator for IT devices on the m-th subcarrier of the s-th OFDM symbol. That is, $b_{n,m,s}=1$ if the m-th subcarrier of the s-th OFDM symbol is allocated to IT device n and $b_{n,m,s}=0$ otherwise. Consequently, we have $\sum_{n=1}^{N} b_{n,m,s} + o_{m,s} \leq 1$ for all m,s. In the following, we describe the over-the-air FL and IT models in detail.

B. Over-the-Air FL Model

We consider an over-the-air FL system, where the learning model is represented by a d-dimensional model parameter vector $\mathbf{w} \in \mathbb{R}^{d \times 1}$. Each FL device k holds its local dataset \mathcal{D}_k of

size $D_k \triangleq |\mathcal{D}_k|$. Let $D \triangleq \sum_{k=1}^K D_k$ denote the total number of training samples. We intend to minimize an empirical loss function of w given by

$$F(\mathbf{w}) = \sum_{k=1}^{K} \rho_k F_k(\mathbf{w}; \mathcal{D}_k), \tag{1}$$

where

$$F_k(\mathbf{w}; \mathcal{D}_k) = \frac{1}{D_k} \sum_{\mathbf{u} \in \mathcal{D}_k} f(\mathbf{w}; \mathbf{u})$$
 (2)

is the local loss function with respect to the local dataset \mathcal{D}_k , $\rho_k \triangleq \frac{D_k}{D}$ is the corresponding weight of $F_k(\cdot)$, and $f(\mathbf{w}; \mathbf{u})$ is the loss function with respect to the local training sample \mathbf{u} .

To minimize (1), the FL devices iteratively update the global model w via distributed stochastic gradient descent (SGD) with T communication rounds. Specifically, the t-th communication round, $0 \le t \le T - 1$, consists of the following steps:

- 1) Model broadcasting: The AP broadcasts the current global model \mathbf{w}_t to all the FL devices in \mathcal{K} .
- 2) Local model updating: Each FL device k parallelly updates the local model by minimizing (2) via a τ -step SGD. Specifically, the l-th step of local SGD, $1 \le l \le \tau$, updates the local model as

$$\mathbf{w}_{k,t}^{l+1} = \mathbf{w}_{k,t}^{l} - \lambda_t \nabla F_k(\mathbf{w}_{k,t}^{l}, \xi_{k,t}^{l}), \tag{3}$$

where $\mathbf{w}_{k,t}^1 = \mathbf{w}_t$, λ_t is the learning rate in the t-th round, and $\nabla F_k(\mathbf{w}_{k,t}^l, \xi_{k,t}^l) \in \mathbb{R}^{d \times 1}$ is the gradient of $F_k(\cdot)$ with respect to the local mini batch $\xi_{k,t}^l \subseteq \mathcal{D}_k$ of size B. Here, each mini batch $\xi_{k,t}^l$ is uniformly drawn from \mathcal{D}_k without replacement. After the τ -step local update, each FL device k computes its local model change $\Delta_{k,t} \triangleq \mathbf{w}_{k,t}^{\tau+1} - \mathbf{w}_t$.

3) Over-the-air model aggregation: All the FL devices concurrently upload the local model changes $\{\Delta_{k,t}\}$ to the AP. The AP estimates the weighted sum $\mathbf{r}_t \triangleq \sum_{k=1}^K \rho_k \Delta_{k,t}$ by exploiting the signal-superposition property of wireless multiple-access channels and updates the global model \mathbf{w}_{t+1} as

$$\mathbf{w}_{t+1} = \mathbf{w}_t + \hat{\mathbf{r}}_t, \tag{4}$$

where $\hat{\mathbf{r}}_t$ is the noisy estimate and $\hat{\mathbf{r}}_t \neq \mathbf{r}_t$ due to the inevitable communication noise.

After T communication rounds, we compute the weighted moving average of $\{\mathbf w_t: t=0,\cdots,T-1\}$ as [25]

$$\hat{\mathbf{w}}_T \triangleq \frac{1}{S_T} \sum_{t=0}^{T-1} \eta_t \mathbf{w}_t, \tag{5}$$

where η_t is the weight of the t-th round, and $S_T \triangleq \sum_{t=0}^{T-1} \eta_t$.

In this paper, we assume perfect downlink model broadcasting following [9]–[12], [23], [32] and focus on the uplink communication design for over-the-air model aggregation, which is elaborated as follows.

With over-the-air model aggregation, we need d RBs in each communication round to upload the d-dimensional vectors $\{\Delta_{k,t}\}$ as each entry occupies one RB. Consequently, over-the-air FL requires dT RBs in total to complete T rounds of model aggregation. We define $\Phi \triangleq \{(m,s): o_{m,s}=1, \forall m \in \mathcal{M}, s \in \mathcal{S}\}$ as the set of indices of all the subcarriers allocated to over-the-air FL, where $|\Phi|=dT$. We partition Φ into T disjoint d-dimensional vectors, where the t-th vector Φ_t denotes the RB indices assigned to the t-th model aggregation round. For example, the first d RBs in Φ is grouped as Φ_1 . We denote the entries of Φ_t by $\Phi_t \triangleq [\Phi[dt+1], \cdots, \Phi[d(t+1)]]^T$. In the t-th model aggregation round, the local model change vector of device k, Δ_t , $\epsilon \in \mathbb{R}^{d \times 1}$ is

In the t-th model aggregation round, the local model change vector of device k, $\Delta_{k,t} \in \mathbb{R}^{d \times 1}$, is first transformed into a normalized transmit symbol vector $\mathbf{x}_{k,t} \in \mathbb{R}^{d \times 1}$ such that $\mathbb{E}[\mathbf{x}_{k,t}\mathbf{x}_{k',t}^H] = \mathbf{0}$ and $\mathbb{E}[\mathbf{x}_{k,t}\mathbf{x}_{k,t}^H] = \mathbf{I}_d, \forall k, k' \in \mathcal{K}, k \neq k'$. Specifically, we first compute the local mean and variance of the local model change $\Delta_{k,t}$ at each FL device k by

$$\overline{\Delta}_{k,t} = \frac{1}{d} \sum_{i=1}^{d} \Delta_{k,t}[i], \quad \nu_{k,t}^2 = \frac{1}{d} \sum_{i=1}^{d} \left(\Delta_{k,t}[i] - \overline{\Delta}_{k,t} \right)^2, \tag{6}$$

where $\Delta_{k,t}[i]$ is the *i*-th entry of $\Delta_{k,t}$. Then, each FL device k uploads its local statistics $\overline{\Delta}_{k,t}$ and $\nu_{k,t}^2$ to the AP and computes

$$x_{k,t}[i] = \frac{\Delta_{k,t}[i] - \overline{\Delta}_{k,t}}{\nu_{k,t}},\tag{7}$$

where $x_{k,t}[i]$ is the *i*-th entry of $\mathbf{x}_{k,t}$. Let $h_{k,m,s} \in \mathbb{C}$ denote the channel coefficient between FL device k and the AP on the m-th subcarrier of the s-th OFDM symbol, and $p_{k,m,s} \in \mathbb{C}$ denote the transmit scalar at FL device k on the m-th subcarrier of the s-th OFDM symbol. The channel coefficient and transmit scalar for transmitting $x_{k,t}[i]$ over the RB indexed by $\Phi_t[i]$ are denoted by $h_{k,\Phi_t[i]}$ and $p_{k,\Phi_t[i]}$, respectively. Let P_1 denote the maximum transmit power of each FL device on each subcarrier. The transmit power at each FL device is constrained by

$$\mathbb{E}\left[|p_{k,\Phi_t[i]}x_{k,t}[i]|^2\right] = |p_{k,\Phi_t[i]}|^2 \le P_1, \quad \forall k \in \mathcal{K}, \Phi_t[i]. \tag{8}$$

We denote the received signal vector at the AP in the t-th round by $\mathbf{y}_t = [y_t[1], \dots, y_t[d]]^T$, with the i-th entry being

$$y_t[i] = \sum_{k=1}^{K} h_{k,\Phi_t[i]} p_{k,\Phi_t[i]} x_{k,t}[i] + z_t[i],$$
(9)

where $z_t[i] \sim \mathcal{CN}(0, \sigma^2)$ is the additive white Gaussian noise (AWGN) with variance σ^2 . The AP estimates the weighted sum $\sum_{k=1}^K \rho_k \Delta_{k,t}[i]$ from $y_t[i]$ by a linear estimator as

$$\hat{r}_{t}[i] = c_{t}[i]y_{t}[i] + \overline{\Delta}_{t} = c_{t}[i] \sum_{k=1}^{K} \frac{h_{k,\Phi_{t}[i]}p_{k,\Phi_{t}[i]}}{\nu_{k,t}} \left(\Delta_{k,t}[i] - \overline{\Delta}_{k,t}\right) + c_{t}[i]z_{t}[i] + \overline{\Delta}_{t},$$
(10)

¹Model compression by, e.g., gradient sparsification [22]–[24], can further reduce the dimensionality of local model changes. Note that our design is readily applicable to any over-the-air FL design that applies gradient sparsification by replacing the model change vectors with the sparsified gradient vectors. Accordingly, the total number of RBs for over-the-air model aggregation is reduced from dT to d'T, where d' < d represents the dimension of compressed local gradient vectors.

where $c_t[i] \in \mathbb{C}$ is the de-noising multiplicative scalar and $\overline{\Delta}_t \triangleq \sum_{k=1}^K \rho_k \overline{\Delta}_{k,t}$ is used for denormalization. With (10), the AP collects $\hat{\mathbf{r}}_t = [\hat{r}_t[1], \cdots, \hat{r}_t[d]]$ and updates the global model by (4).

C. IT Model

As over-the-air FL requires dT RBs in total, the remaining MS - dT RBs are assigned to IT devices for uplink data transmissions, where each RB is allocated to one IT device. Let $g_{n,m,s} \in \mathbb{C}$ denote the channel coefficient between IT device n and the AP on the m-th subcarrier of the s-th OFDM symbol. Then, the corresponding received signal on the m-th subcarrier of the s-th OFDM symbol can be expressed as

$$y_{m,s} = \sum_{n=1}^{N} b_{n,m,s} g_{n,m,s} \sqrt{P_2} x_{n,m,s} + z_{m,s},$$
(11)

where $x_{n,m,s}$ is the digitally-modulated transmit signal with $\mathbb{E}[|x_{n,m,s}|^2] = 1$, P_2 is the transmit power of each IT device, and $z_{m,s} \sim \mathcal{CN}(0,\sigma^2)$ is the AWGN. As a result, the achievable rate of IT device n on the m-th subcarrier of the s-th OFDM symbol is given by

$$R_{n,m,s} = b_{n,m,s} \log_2 \left(1 + \frac{P_2 |g_{n,m,s}|^2}{\phi \sigma^2} \right), \tag{12}$$

where $\phi \geq 1$ is the achievable rate gap due to channel coding and modulation. Consequently, the average IT sum-rate on each OFDM RB is given by

$$R_{\text{avg}} = \frac{1}{MS} \sum_{s=1}^{S} \sum_{m=1}^{M} \sum_{n=1}^{N} R_{n,m,s} = \frac{1}{MS} \sum_{s=1}^{S} \sum_{m=1}^{M} \sum_{n=1}^{N} b_{n,m,s} \log_2 \left(1 + \frac{P_2 |g_{n,m,s}|^2}{\phi \sigma^2} \right).$$
 (13)

D. Problem Formulation

We consider the joint optimization of radio resource allocation and the hyper-parameters of FL, including the number of communication rounds T and the number of local updates τ . To facilitate the problem formulation, we first introduce the definition of an ϵ -accurate solution to characterize the ultimate target of FL model training.

Definition 1 (ϵ -accurate solution). The output of the FL training process $\hat{\mathbf{w}}_T$ is an ϵ -accurate solution to the FL loss minimization problem $\min_{\mathbf{w}} F(\mathbf{w})$ if

$$F(\hat{\mathbf{w}}_T) - F^* \le \epsilon, \tag{14}$$

where $F^* \triangleq F(\mathbf{w}^*)$, \mathbf{w}^* is the global optimum of $F(\cdot)$, and $\epsilon > 0$ is a given positive small number.

The value of ϵ in (14) measures the tolerance of FL model training. A smaller ϵ leads to a smaller optimality gap and thus a better training performance. We note that the training performance $F(\hat{\mathbf{w}}_T)$ depends not only on the model aggregation quality but also on the choice of learning hyper-parameters, including the communication rounds T and the number of local updates τ . In particular, as discussed in the Introduction, the value of τ determines

the computation-to-communication ratio and critically impacts T to achieve a certain training performance. Furthermore, a larger T implies more RBs needed for over-the-air FL training, leaving fewer RBs for data transmissions of IT devices.

Besides the learning hyper-parameters τ and T, the FL training performance and the IT data rate are both affected by the wireless channel fading and thus depend on the subcarrier allocation decisions. However, we highlight that FL and IT have different sensitivities to communication quality. While the effect of the channel coefficients on the IT data rate is given in (13), FL gradient descent is shown to be relatively robust against model aggregation error induced by communication noise and wireless channel fading [33]. This is because a small model aggregation error only slightly perturbs the gradient vector, and the resultant descent direction is still correct for minimizing the loss function with high probability. Motivated by this, we prefer to allocate the subcarriers to IT if the IT devices have good channel conditions and use the remaining radio resources for FL model aggregation. To this end, we propose to maximize the IT data rate and at the same time constrain the expected output of the FL training process to be ϵ -accurate in S symbol durations. Note that the FL subcarrier allocation affects the FL communication rounds T, and hence is coupled with the IT subcarrier allocation. By taking the communication variables $\{b_{n,m,s}, o_{m,s}, p_{k,\Phi_t[i]}, c_t[i]\}$ and the learning hyper-parameters $\{T, \tau\}$ into account, we formulate the CFLIT system optimization problem as:

(P1):
$$\max_{\substack{\{b_{n,m,s},o_{m,s},T,\tau\}\\\{p_{k,\Phi_{t}[i]},c_{t}[i]\}}} R_{\text{avg}}$$
 (15a)

s.t.
$$\mathbb{E}\left[F(\hat{\mathbf{w}}_T; \tau) - F^*\right] \le \epsilon,$$
 (15b)

$$\sum_{s=1}^{S} \sum_{m=1}^{M} o_{m,s} \ge dT, \tag{15c}$$

$$\sum_{n=1}^{N} b_{n,m,s} + o_{m,s} \le 1, \forall m, s, \tag{15d}$$

$$b_{n,m,s} \in \{0,1\}, \forall n, m, s,$$
 (15e)

$$o_{m,s} \in \{0,1\}, \forall m, s,$$
 (15f)

$$|p_{k,\Phi_t[i]}|^2 \le P_1, \forall k \in \mathcal{K}, \Phi_t[i], \tag{15g}$$

$$T, \tau \in \mathbb{Z}^+,$$
 (15h)

where the expectation is taken with respect to the local mini-batch samples, the communication noise, and the channel fading coefficients. $F(\hat{\mathbf{w}}_T; \tau)$ is the achieved training loss after T FL communication rounds with the number of local updates given by τ . In Problem (P1), the constraint (15b) guarantees an ϵ -accurate solution of FL training, (15c) ensures a sufficient number of allocated RBs for over-the-air FL, (15d) implies that each OFDM RB is assigned to

either the over-the-air model aggregation or at most one IT data stream, and (15g) represents the transmit power constraints at FL devices.

The difficulty of solving Problem (P1) is twofold. First, to satisfy the FL convergence requirement in (15b), we must understand how the learning hyper-parameters (T, τ) , the transceiver design variables $\{p_{k,\Phi_t[i]}, c_t[i]\}$, and the subcarrier allocation decisions $\{o_{m,s}\}$ jointly affect the achieved training loss $F(\hat{\mathbf{w}}_T; \tau)$ of over-the-air FL. However, there does not exist an explicit analytical expression to characterize the above coupled impact in the existing literature. This makes it difficult to quantify the required number of RBs for over-the-air model aggregation in advance and minimize it accordingly to optimize the IT performance. Second, to solve (P1) optimally, we need to know the CSI for the entire horizon $s=1,\cdots,S$ at the beginning of time. In practice, however, such non-causal CSI is not available. That is, we need to optimize $\{b_{n,m,s},o_{m,s}\}$ for each symbol duration s based on the instantaneous CSI that is observed at that time. Therefore, an online RB allocation scheme that only depends on the current channel coefficients is required. In the next section, we analyze the performance of over-the-air FL with an arbitrary choice of (T, τ) under mild assumptions on the learning model. To minimize the radio resource consumption of over-the-air FL, we optimize the transceiver design variables $\{p_{k,\Phi_t[i]},c_t[i]\}$ and use the analytical result to compute the optimal solution of (T,τ) to (P1) in the asymptotic regime. Then, in Section IV, we propose a low-complexity online algorithm for subcarrier allocation and analyze its performance.

III. CONVERGENCE ANALYSIS AND LEARNING OPTIMIZATION

In this section, we analyze the convergence of over-the-air FL. To facilitate the analysis, we first present the assumptions on the local loss functions and analyze the model aggregation error in over-the-air model aggregation. Based on this, we show a sufficient condition for FL convergence and derive an asymptotic upper bound of the learning performance in terms of $\mathbb{E}[F(\hat{\mathbf{w}}_T) - F^*]$. Finally, we use the derived bound to optimize the learning hyper-parameters τ and T.

A. Assumptions and Preliminaries

We make the following assumptions on the local loss functions F_1, \dots, F_K :

Assumption 1: F_1, \dots, F_K are all μ -strongly convex, i.e., $\forall \mathbf{w}, \mathbf{w}' \in \mathbb{R}^{d \times 1}$,

$$F_k(\mathbf{w}) \ge F_k(\mathbf{w}') + (\mathbf{w} - \mathbf{w}')^T \nabla F_k(\mathbf{w}') + \frac{\mu}{2} \|\mathbf{w} - \mathbf{w}'\|_2^2.$$
(16)

Assumption 2: F_1, \dots, F_K are all L-smooth, i.e., $\forall \mathbf{w}, \mathbf{w}' \in \mathbb{R}^{d \times 1}$,

$$F_k(\mathbf{w}) \le F_k(\mathbf{w}') + (\mathbf{w} - \mathbf{w}')^T \nabla F_k(\mathbf{w}') + \frac{L}{2} \|\mathbf{w} - \mathbf{w}'\|_2^2.$$
(17)

Assumption 3: The expected l_2 -norm of the stochastic gradient $\nabla F_k(\mathbf{w}_{k,t}^l, \xi_{k,t}^l)$ is upper bounded, i.e., $\forall k, t, l$,

$$\mathbb{E}[\|\nabla F_k(\mathbf{w}_{k,t}^l, \xi_{k,t}^l)\|_2^2] \le G^2,\tag{18}$$

where the expectation is taken with respect to the local mini-batch samples, the communication noise, and the channel fading coefficients.

<u>Remark</u> 3.1: The above assumptions are commonly adopted in the literature; see, e.g., [25], [27], [29]. In practice, Assumption 3 can be guaranteed by imposing an additional gradient clipping operation [34].

The following definition defines a metric of data heterogeneity.

Definition 2 (Γ -data heterogeneity). The degree of data heterogeneity across the FL devices is quantified by

$$\Gamma \triangleq F^* - \sum_{k=1}^K \rho_k F_k^*,\tag{19}$$

where F_k^* denotes the minimum value of local loss function at FL device k, i.e., $F_k(\cdot)$, and $\Gamma \geq 0$.

Note that the value of Γ in (19) approaches zero for i.i.d. data distribution as the number of training samples increases. For non-i.i.d. data distribution, $\Gamma \neq 0$. The larger Γ , the more heterogeneous the data distribution is.

As shown in Section II-B, over-the-air model aggregation constructs a noisy estimate $\hat{\mathbf{r}}_t$ at the AP using (10). The estimation accuracy of $\hat{\mathbf{r}}_t$ affects the convergence of over-the-air FL because the estimation error leads to inaccurate global model update. We quantify the estimation accuracy by the MSE between $\hat{\mathbf{r}}_t$ and the ground-truth \mathbf{r}_t as

$$e_t = \mathbb{E}[\|\hat{\mathbf{r}}_t - \mathbf{r}_t\|_2^2],\tag{20}$$

where the expectation is taken with respect to the communication noise.

It is shown in [7] that a larger model aggregation error e_t leads to a smaller convergence rate of over-the-air FL. Therefore, we can optimize the transceiver design variables $\{p_{k,\Phi_t[i]}, c_t[i]\}$ by minimizing e_t , as detailed by the following lemma.

<u>Lemma</u> 3.1: Given the channel coefficients $\{h_{k,\Phi_t[i]}\}$, the optimal $p_{k,\Phi_t[i]}$ and $c_t[i]$ are

$$p_{k,\Phi_{t}[i]} = \frac{\rho_{k}\nu_{k,t}}{c_{t}[i]h_{k,\Phi_{t}[i]}}, \ \forall k \in \mathcal{K}, \qquad c_{t}[i] = \frac{1}{\sqrt{P_{1}}} \max_{k \in \mathcal{K}} \frac{\rho_{k}\nu_{k,t}}{|h_{k,\Phi_{t}[i]}|}.$$
(21)

Moreover, the minimum e_t is given by

$$e_t = \frac{\sigma^2}{P_1} \sum_{i=1}^d \max_{k \in \mathcal{K}} \frac{\rho_k^2 \nu_{k,t}^2}{|h_{k,\Phi_t[i]}|^2}.$$
 (22)

Proof: See Appendix A.

Lemma 3.1 gives the optimal solution to $\{p_{k,\Phi_t[i]}, c_t[i]\}$ and the analytical expression of the minimum model aggregation error e_t for given channel coefficients $\{h_{k,\Phi_t[i]}\}$. To facilitate the

convergence analysis, we need a tractable expression for the model aggregation error e_t that is independent of the instantaneous channel coefficients. Based on Lemma 3.1 and Assumption 3, we obtain an upper bound of the expected value of e_t in the following lemma.

Lemma 3.2: With Assumption 3, we have

$$\mathbb{E}[e_t] \le \lambda_t^2 \frac{\tau^2 G^2 \sigma^2}{P_1} \mathbb{E}\left[\max_{k \in \mathcal{K}} \frac{\rho_k^2}{|h_k|^2}\right],\tag{23}$$

where the expectations are taken with respect to the local mini-batch samples and the channel fading coefficients, and $\{h_k, \forall k \in \mathcal{K}\}$ are *virtual* i.i.d. random variables following the Gaussian distribution of $\mathcal{CN}(0,1)$.

B. Convergence Result

With Lemma 3.2 and Assumptions 1-3, we derive an upper bound of $\mathbb{E}[F(\hat{\mathbf{w}}_T) - F^*]$ in the following theorem.

<u>Theorem</u> 3.1: Let the learning rate $\lambda_t = \frac{8}{\mu \tau (\gamma + t)}$ and the corresponding weight of the t-th global model $\eta_t = (\gamma + t)^2$ with $\gamma \geq \frac{16L}{\mu}$. With Assumptions 1-3, we have

$$\mathbb{E}[F(\hat{\mathbf{w}}_{T}) - F^{*}] \leq \frac{8T(T + 2\gamma)}{\mu S_{T}} \left(\frac{2\tau^{2} + 1}{3\tau} G^{2} + \frac{4L\Gamma}{\tau} + \frac{G^{2}\sigma^{2}}{P_{1}} \mathbb{E}\left[\max_{k \in \mathcal{K}} \frac{\rho_{k}^{2}}{|h_{k}|^{2}} \right] \right) + \frac{\mu \gamma^{3}}{4S_{T}} \mathbb{E}[\|\mathbf{w}_{0} - \mathbf{w}^{*}\|_{2}^{2}], \quad (24)$$

where S_T is defined in (5), and the expectations are taken with respect to the local mini-batch samples, the communication noise, and the channel fading coefficients.

From Theorem 3.1, we see that $\mathbb{E}[F(\hat{\mathbf{w}}_T) - F^*]$ has an upper bound related to the term $\mathbb{E}\left[\max_{k \in \mathcal{K}} \frac{\rho_k^2}{|h_k|^2}\right]$, which refers to the expected model aggregation error. Since the expected error is independent of the instantaneous channel coefficients $\{h_{k,\Phi_t[i]}\}$, the result in Theorem 3.1 applies to any subcarrier allocation scheme. However, Theorem 3.1 does not explicitly reveal the effect of τ and T. To this end, we further characterize the convergence behavior of $\mathbb{E}[F(\hat{\mathbf{w}}_T) - F^*]$ in the large-system limit, i.e., $T \to \infty$, in the following corollary.

Corollary 3.1: Suppose that the assumptions and conditions in Theorem 3.1 hold. We have

$$\mathbb{E}[F(\hat{\mathbf{w}}_T) - F^*] \le \frac{\zeta(\tau)}{T} + \frac{2\gamma\zeta(\tau)}{T^2} + \frac{3\mu\gamma^3\mathbb{E}[\|\mathbf{w}_0 - \mathbf{w}^*\|_2^2]}{4T^3},\tag{25}$$

where

$$\zeta(\tau) \triangleq \frac{24}{\mu} \left(\frac{2\tau^2 + 1}{3\tau} G^2 + \frac{4L\Gamma}{\tau} + \frac{G^2 \sigma^2}{P_1} \mathbb{E} \left[\max_{k \in \mathcal{K}} \frac{\rho_k^2}{|h_k|^2} \right] \right). \tag{26}$$

Moreover, when T is sufficiently large, i.e., $T \to \infty$, the last two terms on the right hand side (r.h.s.) of (25) are diminishing as $\frac{1}{T^2}, \frac{1}{T^3} \to 0$. In this case, we can approximate the upper bound of $\mathbb{E}[F(\hat{\mathbf{w}}_T) - F^*]$ as

$$\mathbb{E}[F(\hat{\mathbf{w}}_T) - F^*] \le \frac{\zeta(\tau)}{T} + O\left(\frac{1}{T^2}\right) \approx \frac{\zeta(\tau)}{T} \quad \text{as} \quad T \to \infty.$$
 (27)

Proof: Since
$$S_T = \sum_{t=0}^{T-1} \eta_t = \sum_{t=0}^{T-1} (\gamma + t)^2$$
 and $\gamma \ge \frac{16L}{\mu} \ge 1$, we have

$$S_T = \sum_{t=0}^{T-1} \gamma^2 + 2\gamma t + t^2 = \gamma^2 T + \gamma T(T-1) + \frac{T(T-1)(2T-1)}{6} \ge \frac{1}{3}T^3.$$
 (28)

Plugging this result into (24), we obtain (25).

From Corollary 3.1, we see that the output of the FL training process $\hat{\mathbf{w}}_T$ guarantees to converge to the global optimum and over-the-air FL has a convergence rate of $O(\frac{1}{T})$ for a sufficiently large T. Moreover, as shown in (27), the asymptotic upper bound in the large-system limit is a function of the learning hyper-parameters τ and T. Since T is sufficiently large in practice, we use the upper bound in (27) as an approximation of $\mathbb{E}[F(\hat{\mathbf{w}}_T) - F^*]$, i.e., $\mathbb{E}[F(\hat{\mathbf{w}}_T) - F^*] \approx \frac{\zeta(\tau)}{T}$, and asymptotically optimize τ and T in the next subsection.

C. Optimization of Learning Parameters

To obtain an ϵ -accurate solution, i.e., to achieve $\mathbb{E}[F(\hat{\mathbf{w}}_T) - F^*] \leq \epsilon$, it is sufficient to ensure $\frac{\zeta(\tau)}{T} \leq \epsilon$, which yields

$$T \ge \frac{\zeta(\tau)}{\epsilon} = \frac{24}{\mu\epsilon} \left(\frac{2G^2}{3}\tau + \frac{G^2 + 12L\Gamma}{3\tau} + \frac{G^2\sigma^2}{P_1} \mathbb{E}\left[\max_{k \in \mathcal{K}} \frac{\rho_k^2}{|h_k|^2} \right] \right). \tag{29}$$

From (29), we see that T is lower bounded by a function of τ , which is not monotonic. Specifically, the r.h.s. of (29) first decreases and then increases with τ , showing that the minimizer of $\zeta(\tau)$ exists. Note that we can equivalently minimize the radio resource consumption of overthe-air FL by minimizing the required communication rounds T. To obtain the minimum T^* , it suffices to find the optimal τ^* that minimizes $\zeta(\tau)$, i.e., $\tau^* = \arg\min \zeta(\tau)$, which is equivalent to solving the following optimization problem:

$$\min_{\tau} \quad \psi(\tau) = \frac{2G^2}{3}\tau + \frac{G^2 + 12L\Gamma}{3\tau}$$
 (30a)

s.t.
$$\tau \in \mathbb{Z}^+, \tau \ge 1$$
, (30b)

where the objective function $\psi(\tau)$ is derived from $\zeta(\tau)$ by omitting the constant term.

Problem (30) is an one-dimensional integer programming problem and can be solved optimally as follows. Specifically, we first solve the following relaxed problem:

$$\min_{\tau \in \mathbb{R}, \tau \ge 1} \quad \psi(\tau) = \frac{2G^2}{3}\tau + \frac{G^2 + 12L\Gamma}{3\tau}.$$
 (31)

Since Problem (31) is convex, the optimal solution is given by

$$\tau_{\text{relax}} = \max\left\{1, \sqrt{\frac{1}{2} + \frac{6L\Gamma}{G^2}}\right\}. \tag{32}$$

Then, the optimal solution τ^* to Problem (30) can be obtained by simply rounding (32) as

$$\tau^* = \underset{\tau \in \{ \lfloor \tau_{\text{relax}} \rfloor, \lceil \tau_{\text{relax}} \rceil \}}{\operatorname{argmin}} \psi(\tau), \tag{33}$$

where $\lfloor \cdot \rfloor$ denotes the floor function, and $\lceil \cdot \rceil$ denotes the ceiling function.

Substituting the optimal value of τ^* in (33) into (29), we have

$$T \ge \frac{\zeta(\tau^*)}{\epsilon} = \frac{24}{\mu\epsilon} \left(\frac{2G^2}{3} \tau^* + \frac{G^2 + 12L\Gamma}{3\tau^*} + \frac{G^2\sigma^2}{P_1} \mathbb{E} \left[\max_{k \in \mathcal{K}} \frac{\rho_k^2}{|h_k|^2} \right] \right). \tag{34}$$

As $T \in \mathbb{Z}^+$, the minimum T^* satisfying (34) is given by

$$T^* = \left[\frac{24}{\mu \epsilon} \left(\frac{2G^2}{3} \tau^* + \frac{G^2 + 12L\Gamma}{3\tau^*} + \frac{G^2 \sigma^2}{P_1} \mathbb{E} \left[\max_{k \in \mathcal{K}} \frac{\rho_k^2}{|h_k|^2} \right] \right) \right]. \tag{35}$$

We see from (32) and (35) that the large-system asymptotic results τ^* and T^* depend on the parameters L, Γ , and G, which are determined by the data distribution and the learning task. The accuracy of the derived $\{\tau^*, T^*\}$ is verified by numerical results in Section V.

IV. ONLINE SUBCARRIER ALLOCATION FOR CFLIT

We have discussed the optimization of $\{T, \tau, p_{k,\Phi_t[i]}, c_t[i]\}$ in Section III. The remaining challenge of solving Problem (P1) lies in optimizing the binary subcarrier allocation variables $\{b_{n,m,s}, o_{m,s}\}$ without the non-causal CSI. In this section, we propose a low-complexity threshold-based online algorithm that only requires the CSI in the current symbol duration s to optimize $\{b_{n,m,s}, o_{m,s}\}$ in an online manner. Furthermore, we analyze the achievable performance of the proposed algorithm.

A. Threshold-Based Online Subcarrier Allocation

As discussed in Section III, our analysis of FL convergence does not rely on the instantaneous CSI of FL devices. Moreover, the channel coefficients of FL devices are independent of those of IT devices. Therefore, the convergence analysis in Section III is applicable to arbitrary subcarrier allocation. With the optimized $\{T, \tau, p_{k,\Phi_t[i]}, c_t[i]\}$, the FL convergence requirement in (15c) can be satisfied by ensuring that the number of allocated subcarriers for over-the-air FL is sufficiently large to complete T^* rounds of model aggregation. Accordingly, Problem (P1) is simplified as:

(P2):
$$\max_{\{b_{n,m,s},o_{m,s}\}} R_{\text{avg}} = \frac{1}{MS} \sum_{s=1}^{S} \sum_{m=1}^{M} \sum_{n=1}^{N} b_{n,m,s} \log_2 \left(1 + \frac{P_2 |g_{n,m,s}|^2}{\phi \sigma^2} \right)$$
(36a)

s.t.
$$\sum_{s=1}^{S} \sum_{m=1}^{M} o_{m,s} \ge dT^*, \tag{36b}$$

$$\sum_{n=1}^{N} b_{n,m,s} + o_{m,s} \le 1, \forall m, s, \tag{36c}$$

$$b_{n,m,s} \in \{0,1\}, \forall n, m, s,$$
 (36d)

$$o_{m,s} \in \{0,1\}, \forall m, s.$$
 (36e)

We note that the subcarrier allocation is independent of the channel coefficients of FL devices $\{h_{k,m,s}\}$, as implied by (36a) and (36b). Intuitively, once the CSI of the entire time horizon is available, we can simply obtain the offline optimal solution to Problem (P2). Specifically, we can pick the best $MS-dT^*$ subcarriers across the S symbol durations and assign each of them to the IT device with the best channel condition for rate maximization. In practice, however, such CSI

is unavailable in advance. This makes it difficult to exactly find these globally best subcarriers in each symbol duration. In the following, we propose a threshold-based online subcarrier allocation algorithm that only requires the current CSI to mimic the offline optimal solution.

To begin with, we denote the highest channel gain among all IT devices on the m-th subcarrier of the s-th OFDM symbol by $\bar{g}_{m,s}$ as

$$\bar{g}_{m,s} = \max_{n \in \mathcal{N}} \left\{ |g_{1,m,s}|^2, \cdots, |g_{n,m,s}|^2, \cdots, |g_{N,m,s}|^2 \right\}.$$
(37)

Since the channel coefficient $g_{n,m,s}$ follows the i.i.d. complex Gaussian distribution of $\mathcal{CN}(0,1)$, the channel gain $|g_{n,m,s}|^2$, $\forall n,m,s$, follows the i.i.d. chi-squared distribution with 2 degrees of freedom, i.e., $|g_{n,m,s}|^2 \sim \chi^2(2)$, whose cumulative distribution function (CDF) is specified by

$$F_{|g_{n,m,s}|^2}(x) = P(|g_{n,m,s}|^2 \le x) = 1 - e^{-x}.$$
 (38)

With (38), the CDF of $\bar{g}_{m,s}$ is

$$F_{\bar{g}_{m,s}}(x) = P(\bar{g}_{m,s} \le x) = \prod_{n=1}^{N} F_{|g_{n,m,s}|^2}(x) = (1 - e^{-x})^N.$$
(39)

Furthermore, the probability density function (PDF) of $\bar{g}_{m,s}$ can be calculated as

$$f_{\bar{g}_{m,s}}(x) = \frac{dF_{\bar{g}_{m,s}}(x)}{dx} = \begin{cases} Ne^{-x}(1 - e^{-x})^{N-1}, & x \ge 0, \\ 0, & \text{otherwise.} \end{cases}$$
(40)

Let p_{IT} denote the proportion of subcarriers allocated to IT devices in the entire time horizon. According to the offline optimal solution, we have

$$p_{\rm IT} = \frac{MS - dT^*}{MS}. (41)$$

To mimic the offline optimal subcarrier allocation, we can derive a threshold of $\{\bar{g}_{m,s}\}$, denoted by q, such that the expected proportion of subcarriers allocated to IT is p_{IT} . Specifically, a subcarrier is allocated to IT if the corresponding $\bar{g}_{m,s}$ exceeds the threshold q and allocated to over-the-air model aggregation otherwise. To this end, we employ the *quantile function* of $\bar{g}_{m,s}$ to compute q as

$$q = Q_{\bar{g}_{m,s}}(1 - p_{\text{IT}}) = \inf\{x \in \mathbb{R} : 1 - p_{\text{IT}} \le F_{\bar{g}_{m,s}}(x)\} = -\ln\left(1 - \sqrt[N]{1 - p_{\text{IT}}}\right). \tag{42}$$

Then, the online subcarrier allocation solution to (P2) is given by

$$o_{m,s} = \begin{cases} 1, & \bar{g}_{m,s} < q, \\ 0, & \text{otherwise,} \end{cases} \text{ and } b_{n,m,s} = \begin{cases} 1, & \bar{g}_{m,s} \ge q \text{ and } n = \underset{n' \in \mathcal{N}}{\operatorname{argmax}} |g_{n',m,s}|^2, \\ 0, & \text{otherwise.} \end{cases}$$
(43)

We summarize the proposed threshold-based online subcarrier allocation algorithm in Algorithm 1. We initialize $o_{m,s}=1$, $b_{n,m,s}=0$, $\forall n$ for all subcarriers and introduce an auxiliary variable I_{total} to denote the accumulated number of subcarriers allocated to IT. If the number of allocated subcarriers for FL achieves its maximum value dT^* , the remaining RBs will be allocated to IT; see Lines 7-8. By doing this, the proposed algorithm allocates exactly dT^* subcarriers to over-the-air FL, guaranteeing that the solution is always feasible to Problem (P2).

Algorithm 1 Threshold-Based Online Subcarrier Allocation Algorithm

```
1: Input: T^*; d; S; M; N;
 2: Initialization: o_{m,s} = 1, \forall m, s; \ b_{n,m,s} = 0, \forall n, m, s; \ p_{\text{IT}} = \frac{MS - dT^*}{MS}; \ q = -\ln(1 - \sqrt[N]{1 - p_{\text{IT}}}); \ I_{\text{total}} = 0;
 3: for s = 1, \dots, S do
          for m=1,\cdots,M do
             if I_{\text{total}} < MS \cdot p_{\text{IT}} then
                  Compute \bar{g}_{m,s} = \max_{n \in \mathcal{N}} |g_{n,m,s}|^2 and n = \operatorname{argmax}_{n' \in \mathcal{N}} |g_{n',m,s}|^2;
 6:
                  if (s-1)M + m - I_{\text{total}} > dT^* then
 7:
                      Update o_{m,s} = 0 and b_{n,m,s} = 1;
 8:
10:
                      Update o_{m,s} and b_{n,m,s} by (43);
11:
                  end if
                  Update I_{\text{total}} = I_{\text{total}} + (1 - o_{m,s});
12:
13:
             end if
         end for
14:
15: end for
16: Output: \{b_{n,m,s}, o_{m,s}\}.
```

Since the complexity of Lines 6-12 is O(N), the computational complexity of allocating each subcarrier is O(N). Therefore, the overall complexity of Algorithm 1 is O(MSN).

B. Performance Analysis

In this subsection, we analyze the performance of the proposed threshold-based online algorithm, i.e., Algorithm 1. Let $\hat{g}_{m,s}$ denote the effective IT channel gain on the m-th subcarrier of the s-th OFDM symbol with the proposed threshold-based subcarrier allocation as

$$\hat{g}_{m,s} = \begin{cases} \bar{g}_{m,s}, & \bar{g}_{m,s} \ge q, \\ 0, & \text{otherwise.} \end{cases}$$
(44)

With (44), the expected objective value achieved by Algorithm 1 is

$$\mathbb{E}[R_{\text{avg}}] = \mathbb{E}\left[\frac{1}{MS} \sum_{s=1}^{S} \sum_{m=1}^{M} \sum_{n=1}^{N} b_{n,m,s} \log_2\left(1 + \frac{P_2|g_{n,m,s}|^2}{\phi\sigma^2}\right)\right] = p_{\text{IT}} \mathbb{E}\left[\log_2\left(1 + \theta \hat{g}_{m,s}\right)\right],\tag{45}$$

where $\theta \triangleq \frac{P_2}{\phi \sigma^2}$ is a known constant. The following proposition gives a closed-form expression of (45).

Proposition 4.1: The expected average IT sum-rate achieved by Algorithm 1 is given by

$$\mathbb{E}[R_{\text{avg}}] = N \sum_{i=0}^{N-1} \frac{\binom{N-1}{i}(-1)^i}{(i+1)\ln 2} \left[\ln (1+\theta q) e^{-(i+1)q} + e^{\frac{i+1}{\theta}} E_1 \left(\frac{i+1}{\theta} + (i+1)q \right) \right], \tag{46}$$

where q is given by (42), and $E_1(z) \triangleq \int_z^\infty \frac{e^{-t}}{t} dt$ is the first-order exponential integral.

We compare the performance of the proposed algorithm with a baseline called random subcarrier allocation (RSCA). Specifically, RSCA randomly allocates each subcarrier to IT with probability $p_{\rm IT}$ and to over-the-air model aggregation with probability $1-p_{\rm IT}$. This results in a suboptimal solution to Problem (P2). We denote the achievable expected objective value of RSCA by

$$\mathbb{E}[\hat{R}_{\text{avg}}] = p_{\text{IT}} \mathbb{E}\left[\log_2\left(1 + \theta \bar{g}_{m,s}\right)\right],\tag{47}$$

and the rate improvement of the proposed algorithm by $\varrho(q) \triangleq \mathbb{E}[R_{\text{avg}}] - \mathbb{E}[\hat{R}_{\text{avg}}]$. The following proposition gives a closed-form expression of $\varrho(q)$.

Proposition 4.2: The expected average IT sum-rate in (47) is given by

$$\mathbb{E}[\hat{R}_{\text{avg}}] = \left[1 - (1 - e^{-q})^{N}\right] N \sum_{i=0}^{N-1} \frac{\binom{N-1}{i}(-1)^{i}}{(i+1)\ln 2} e^{\frac{(i+1)}{\theta}} E_{1}\left(\frac{i+1}{\theta}\right). \tag{48}$$

The rate improvement $\varrho(q)$ is always non-negative with the following closed-form expression:

$$\varrho(q) = N \sum_{i=0}^{N-1} \frac{\binom{N-1}{i}(-1)^i}{(i+1)\ln 2} \left[\ln(1+\theta q)e^{-(i+1)q} + e^{\frac{i+1}{\theta}} E_1 \left(\frac{(i+1)(1+\theta q)}{\theta} \right) + \left((1-e^{-q})^N - 1 \right) e^{\frac{i+1}{\theta}} E_1 \left(\frac{i+1}{\theta} \right) \right]$$

$$\geq 0.$$
 (49)

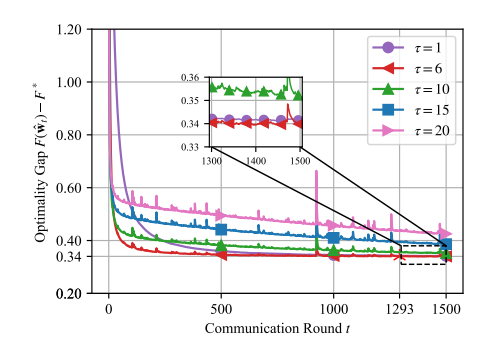
V. NUMERICAL RESULTS

In this section, we conduct experiments to verify our theoretical analysis and evaluate the performance of the proposed design.

A. Experiment Settings

We simulate a single-cell model edge network that comprises one AP, K=20 FL devices, and N=5 IT devices with M=512 OFDM subcarriers. The frequency-selective channel has an exponential power delay profile with a delay spread of 6 taps. Unless otherwise stated, we set S=2000 with each symbol duration equals to $16~\mu s$, $P_1=P_2=1$ W, $\phi=6$ dB, and $\sigma^2=0.1$ W. For over-the-air FL, we consider the regularized logistic regression task with the synthetic dateset specified in [26, Section 5]. Specifically, we generate the local data samples of each device k { $\mathbf{X}_k, \mathbf{y}_k$ } of size D_k according to the model $y=\operatorname{argmax}(\operatorname{softmax}(\mathbf{W}_k\mathbf{x}+\mathbf{b}_k))$, where $\operatorname{softmax}(z_i) \triangleq \frac{e^{z_i}}{\sum_j e^{z_j}}$ is the softmax function, $\mathbf{X}_k \in \mathbb{R}^{D_k \times 60}$, $\mathbf{y}_k \in \mathbb{R}^{D_k \times 1}$, $\mathbf{W}_k \in \mathbb{R}^{10 \times 60}$, $\mathbf{x} \in \mathbb{R}^{60 \times 1}$, and $\mathbf{b}_k \in \mathbb{R}^{10 \times 1}$. We draw each entry of \mathbf{W}_k and \mathbf{b}_k following the distribution of $\mathcal{N}(u_k, 1)$ with $u_k \sim \mathcal{N}(0, \alpha)$, and $(\mathbf{x}_k)_j$ following the distribution of $\mathcal{N}(v_k, \frac{1}{j^{1.2}})$ with $v_k \sim \mathcal{N}(B_k, 1)$ and $B_k \sim \mathcal{N}(0, \beta)$. Here, α and β control the model heterogeneity and data heterogeneity, respectively. In our simulations, we set $\alpha = \beta = 1$ by following [27]. The sizes of local datasets, i.e., { D_k }, are randomly drawn by following a power law distribution [26]. The loss function is given by

$$F(\mathbf{w}) = \frac{1}{D} \sum_{i=1}^{D} \text{CrossEntropy}(f(\mathbf{w}; \mathbf{x}_i), y_i) + \frac{\varphi}{2} ||\mathbf{w}||_2^2,$$
 (50)



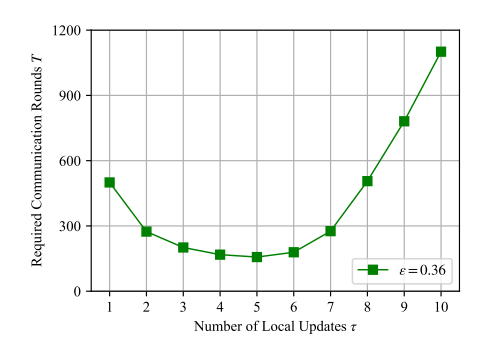


Fig. 2: Optimality gap of different numbers of local updates τ .

Fig. 3: Required T to achieve an ϵ -accurate solution.

where (\mathbf{x}_i, y_i) is the *i*-th data sample, $f(\mathbf{w}; \mathbf{x}_i) \triangleq \operatorname{softmax}(\mathbf{W}\mathbf{x}_i + \mathbf{b})$ is the prediction model with the parameter $\mathbf{w} = (\mathbf{W}, \mathbf{b})$, and $\varphi = 0.5$ is the regularization parameter. To minimize (50), all the FL devices train a common regression model consisting of an input layer and a softmax output layer with the total number of model parameters d equals to 610. We set the mini-batch size B = 32, the local SGD clipping threshold G = 1, the learning rate $\lambda_t = 0.05 \cdot \frac{\gamma}{\gamma + t}$ and the weight of each global model iterate $\eta_t = (\gamma + t)^2$ with $\gamma = 1000$. To verify the analysis, we numerically estimate the values of the learning hyper-parameters as $\Gamma = 0.639, \mu = 0.5, L = 10.25$, and $\mathbb{E}[\max_{k \in \mathcal{K}} \rho_k^2/|h_k|^2] = 1.294$. All the simulation results in this section are averaged over 20 Monte Carlo trials.

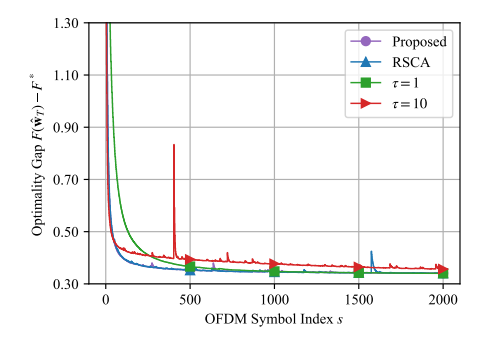
B. Verification of Learning Analysis

We first evaluate the optimality of the learning hyper-parameters τ^* and T^* derived in Section III. In Fig. 2, we plot the optimality gap of over-the-air FL, i.e., $F(\hat{\mathbf{w}}_T) - F^*$, with different values of τ in 1,500 communication rounds. Our analysis in (33) shows that the optimal $\tau^* = 6$, which corresponds to the best learning performance in Fig. 2. We see that $\tau = 1$ leads to a slower convergence rate and a higher final training loss than $\tau = 6$. On the other hand, due to the data heterogeneity, we observe evident performance degradation when $\tau > 6$ as too intensive local updating hurts the global convergence. With $\tau = 6$, it requires T = 1293 rounds to achieve a 0.34-accurate solution, which matches our analytical result $T^* = 1208$ in (35).

In Fig. 3, we study the impact of the number of local updates on the required FL communication rounds T to achieve a 0.36-accurate solution, i.e., $F(\hat{\mathbf{w}}_T) - F^* \leq 0.36$. We see from Fig. 3 that the value of T is sensitive to the choice of τ and their relationship is non-monotonic. This observation coincides with our analysis in Section III. Moreover, the optimal value of τ obtained by the simulation ($\tau^* = 5$) is close to our analysis ($\tau^* = 6$), which verifies the accuracy of our theoretical learning optimization results in Section III.

TABLE I: Average IT sum-rate R_{avg} (Kbps) with S=2000, N=5.

				,	
Scheme	Offline	Proposed	RSCA	$\tau = 1$	$\tau = 10$
$R_{\rm avg}$ (Kbps)	66.40	66.28	52.38	0	53.04



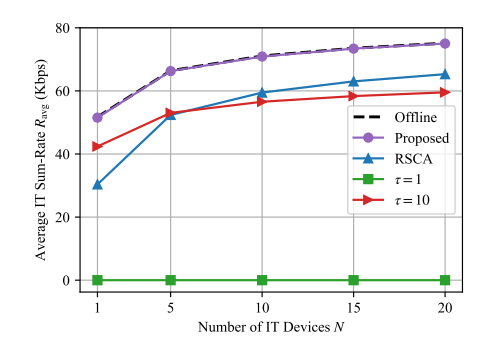


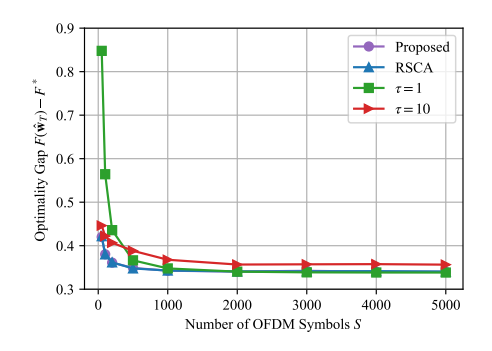
Fig. 4: Optimality gap with S = 2000, N = 5.

Fig. 5: Average IT sum-rate versus N with S = 2000.

C. Simulations on CFLIT Performance

We compare the proposed CFLIT design with four baseline schemes. First, we consider the offline optimal subcarrier allocation scheme described in Section IV-A, where we assume that the non-causal CSI is available beforehand. This ideal baseline characterizes the best IT performance. Second, we consider the RSCA scheme described in Section IV-B, which randomly allocates each RB to IT with probability $p_{\rm IT}$ and to over-the-air FL with probability $1-p_{\rm IT}$. Then, we consider two FL schemes with fixed learning configuration $\tau=1$ and $\tau=10$, where the corresponding subcarrier allocation is optimized by using Algorithm 1. For fair comparison, the numbers of local updates in the proposed scheme and RSCA are both optimized by (33) as $\tau^*=6$. For over-the-air FL, the number of communication rounds is determined offline by (35) with the learning target given by $F(\hat{\mathbf{w}}_T) - F^* \leq \epsilon = 0.36$.

In Table I and Fig. 4, we present the average IT sum-rate and the FL loss, respectively, with S=2000 OFDM symbols. We observe that the proposed online algorithm achieve a comparable average IT sum-rate with the offline scheme. Moreover, the proposed scheme outperforms all the other baselines in terms of both the FL convergence and the IT data rate. Although the optimality gap of the baseline with $\tau=1$ gradually approaches that of the proposed scheme, it fails to serve the IT devices as all the radio resources are used for over-the-air model aggregation. Due to the data heterogeneity, the baseline with $\tau=10$ tends to converge to local optima and requires more FL communication rounds than the proposed scheme, which leads to a worse CFLIT system performance. Thanks to the optimization of τ , the RSCA scheme achieves comparable learning performance with the proposed scheme, but it achieves a lower IT data rate than our proposed method. By joint communication and learning design, the proposed scheme efficiently utilizes the



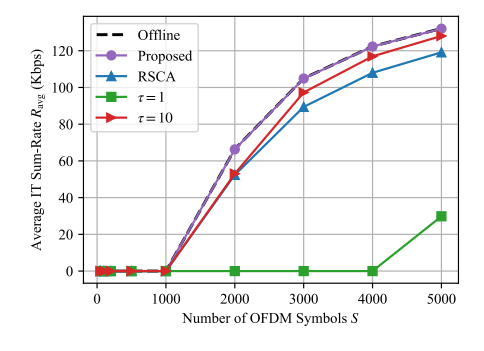


Fig. 6: Optimality gap versus S with N=5.

Fig. 7: Average IT sum-rate versus S with N=5.

limited radio resources and thus provides better performance for the coexistence of over-the-air FL and IT.

In Fig. 5, we study the impact of the number of IT devices N on the average IT sum-rate with S=2000 OFDM symbols. We see that the proposed scheme achieves a similar average IT sum-rate to the offline scheme and outperforms the other baselines. As N increases, the performance gap between the RSCA scheme and the proposed scheme becomes smaller. This is because increasing the number of IT devices improves the effective received signal-to-noise ratio (SNR) for all the schemes. In contrast, the performance of the two baselines with fixed FL design, i.e., $\tau=1$ and $\tau=10$, suffers from slow FL convergence. Consequently, they have much less remaining RBs for uplink IT compared with the proposed scheme.

In Figs. 6 and 7, we study the impact of the number of OFDM symbols S on the FL performance and the average IT sum-rate, respectively. We see that the value of S reflects the availability of radio resources and thus critically affects the performance of both the FL and the IT. Specifically, when S is small, e.g., $S \leq 2000$, the radio resources should be allocated to over-the-air FL to fulfill the convergence requirement, which limits the data rate of IT devices. As S increases, more RBs can be used for uplink data transmissions, leading to a higher IT data rate. As shown in Fig. 7, the propose online algorithm achieves near-optimal IT performance. With efficient exploitation of the learning properties, our proposed design well balances the resource allocation in FL and IT and thus achieves a better performance compared with the other baselines. The above observation verifies the superiority of the proposed design in supporting the coexistence of FL and IT, especially when radio resources are limited.

VI. CONCLUSIONS

In this paper, we proposed a novel CFLIT framework to support the coexistence of over-theair FL and uplink information transfer. To maximize the average IT data rate while ensuring the convergence of over-the-air FL, we studied the joint optimization of the OFDM subcarrier allocation, the transceiver design, and the FL hyper-parameters. We analyzed the convergence of over-the-air FL to minimize the bandwidth consumption needed for FL convergence guarantee. Based on the analysis, we optimized the transceiver design, the number of local updates, and the number of FL communication rounds. Moreover, we proposed a low-complexity online algorithm to optimize the CFLIT subcarrier allocation under the time-varying channels and derived a closed-form expression of its achievable IT data rate. Extensive simulations verify our analysis and demonstrate the performance improvement, in both the FL convergence and the average IT data rate, of the proposed design compared with the baselines.

APPENDIX A

Proof of Lemma 3.1

Substituting (10) into the expression of e_t , we have

$$e_{t} = \mathbb{E}[\|\hat{\mathbf{r}}_{t} - \mathbf{r}_{t}\|_{2}^{2}] = \sum_{i=1}^{d} \mathbb{E}\left[\left|\sum_{k=1}^{K} \left(\frac{c_{t}[i]h_{k,\Phi_{t}[i]}p_{k,\Phi_{t}[i]}}{\nu_{k,t}} - \rho_{k}\right) \left(\Delta_{k,t}[i] - \overline{\Delta}_{k,t}\right)\right|^{2} + |c_{t}[i]z_{t}[i]|^{2}\right]$$

$$\stackrel{(a)}{\geq} \sum_{i=1}^{d} \mathbb{E}\left[|c_{t}[i]z_{t}[i]|^{2}\right] = \sum_{i=1}^{d} |c_{t}[i]|^{2}\sigma^{2},$$
(51)

where the equality in (a) holds if $\frac{c_t[i]h_{k,\Phi_t[i]}p_{k,\Phi_t[i]}}{\nu_{k,t}} - \rho_k = 0, \forall k \in \mathcal{K}$. From [35, eqs. (49)-(54)], we obtain the optimal $p_{k,\Phi_t[i]}$ and $c_t[i]$ as

$$p_{k,\Phi_{t}[i]} = \frac{\rho_{k}\nu_{k,t}}{c_{t}[i]h_{k,\Phi_{t}[i]}}, \quad \forall k \in \mathcal{K}, \qquad c_{t}[i] = \frac{1}{\sqrt{P_{1}}} \max_{k \in \mathcal{K}} \frac{\rho_{k}\nu_{k,t}}{|h_{k,\Phi_{t}[i]}|}.$$
 (52)

Plugging (52) into (51), we obtain the minimum e_t as $e_t = \frac{\sigma^2}{P_1} \sum_{i=1}^d \max_{k \in \mathcal{K}} \frac{\rho_k^2 \nu_{k,t}^2}{|h_{k,\Phi_t[i]}|^2}$.

APPENDIX B

PROOF OF LEMMA 3.2

By taking expectation with respect to the local mini-batch samples and the channel fading coefficients on both sides of (22) and replacing $h_{k,\Phi_t[i]}$, $\forall i$, by h_k , we obtain

$$\mathbb{E}[e_t] = \mathbb{E}\left[\frac{\sigma^2}{P_1} \sum_{i=1}^d \max_{k \in \mathcal{K}} \frac{\rho_k^2 \nu_{k,t}^2}{|h_k|^2}\right] = \mathbb{E}\left[\frac{d\sigma^2}{P_1} \max_{k \in \mathcal{K}} \frac{\rho_k^2 \nu_{k,t}^2}{|h_k|^2}\right],\tag{53}$$

where the last equality is because $\{h_k\}$ are i.i.d. over the index i. For $\forall k \in \mathcal{K}$, we have

$$\mathbb{E}\left[d\rho_{k}^{2}\nu_{k,t}^{2}\right] = \mathbb{E}\left[\rho_{k}^{2}\sum_{i=1}^{d}\left(\Delta_{k,t}[i] - \frac{1}{d}\sum_{i'=1}^{d}\Delta_{k,t}[i']\right)^{2}\right] = \mathbb{E}\left[\rho_{k}^{2}\left(\sum_{i=1}^{d}\Delta_{k,t}^{2}[i] - \frac{1}{d}\left(\sum_{i'=1}^{d}\Delta_{k,t}[i']\right)^{2}\right)\right]$$

$$\stackrel{(a)}{\leq} \mathbb{E}\left[\rho_{k}^{2}\sum_{i=1}^{d}\Delta_{k,t}^{2}[i]\right] = \mathbb{E}\left[\rho_{k}^{2}\left\|-\lambda_{t}\sum_{l=1}^{\tau}\nabla F_{k}(\mathbf{w}_{k,t}^{l},\xi_{k,t}^{l})\right\|_{2}^{2}\right]$$

$$\stackrel{(b)}{\leq} \rho_{k}^{2}\lambda_{t}^{2}\tau\sum_{l=1}^{\tau}\mathbb{E}\left[\left\|\nabla F_{k}(\mathbf{w}_{k,t}^{l},\xi_{k,t}^{l})\right\|_{2}^{2}\right]\stackrel{(c)}{\leq}\rho_{k}^{2}\lambda_{t}^{2}\tau^{2}G^{2}, \quad (54)$$

where (a) is because $(\sum_{i'=1}^{d} \Delta_{k,t}[i'])^2/d \ge 0$, (b) is from the convexity of $\|\cdot\|_2^2$, and (c) is from (18). Plugging (54) into (53) gives (23), which completes the proof.

APPENDIX C

PROOF OF THEOREM 3.1

To prove Theorem 3.1, we first introduce the following lemma.

<u>Lemma</u> C.1: With Assumptions 1-3 and $\lambda_t \leq \frac{1}{2L\tau}$, we have

$$\mathbb{E}[\|\mathbf{w}_{t+1} - \mathbf{w}^*\|_2^2] \le \left(1 - \frac{\mu \lambda_t \tau}{2}\right) \mathbb{E}\left[\|\mathbf{w}_t - \mathbf{w}^*\|_2^2\right] - \frac{1}{2}\lambda_t \tau \mathbb{E}\left[F(\mathbf{w}_t) - F^*\right] + \lambda_t^2 \tau^2 G^2$$

$$+ 2\sum_{k=1}^K \rho_k \sum_{l=2}^{\tau} \mathbb{E}\left[\|\mathbf{w}_{k,t}^l - \mathbf{w}_t\|_2^2\right] + 4\lambda_t^2 \tau L\Gamma + \mathbb{E}\left[\|\hat{\mathbf{r}}_t - \mathbf{r}_t\|_2^2\right]. \tag{55}$$

Proof: See Appendix F.

Since $\mathbf{w}_{k,t}^l - \mathbf{w}_t = -\lambda_t \sum_{j=1}^{l-1} \nabla F_k(\mathbf{w}_{k,t}^j, \xi_{k,t}^j)$, we have

$$\sum_{k=1}^{K} \rho_{k} \sum_{l=2}^{\tau} \mathbb{E} \left[\| \mathbf{w}_{k,t}^{l} - \mathbf{w}_{t} \|_{2}^{2} \right] = \lambda_{t}^{2} \sum_{k=1}^{K} \rho_{k} \sum_{l=2}^{\tau} \mathbb{E} \left[\left\| \sum_{j=1}^{l-1} \nabla F_{k}(\mathbf{w}_{k,t}^{j}, \xi_{k,t}^{j}) \right\|_{2}^{2} \right] \\
\stackrel{(a)}{\leq} \lambda_{t}^{2} \sum_{k=1}^{K} \rho_{k} \sum_{l=2}^{\tau} (l-1) \sum_{j=1}^{l-1} \mathbb{E} \left[\| \nabla F_{k}(\mathbf{w}_{k,t}^{j}, \xi_{k,t}^{j}) \|_{2}^{2} \right] \\
\stackrel{(b)}{\leq} \lambda_{t}^{2} \sum_{k=1}^{K} \rho_{k} \sum_{l=2}^{\tau} (l-1)^{2} G^{2} = \lambda_{t}^{2} \frac{\tau(\tau-1)(2\tau-1)}{6} G^{2}, \tag{56}$$

where (a) is from the convexity of $\|\cdot\|_2^2$, and (b) is from (18).

Moreover, from Lemma 3.2, we have

$$\mathbb{E}[\|\hat{\mathbf{r}}_t - \mathbf{r}_t\|_2^2] \le \lambda_t^2 \frac{\tau^2 G^2 \sigma^2}{P_1} \mathbb{E}\left[\max_{k \in \mathcal{K}} \frac{\rho_k^2}{|h_k|^2}\right]. \tag{57}$$

Substituting (56) and (57) into (55), we have

$$\mathbb{E}[\|\mathbf{w}_{t+1} - \mathbf{w}^*\|_2^2] \le \left(1 - \frac{\mu \lambda_t \tau}{2}\right) \mathbb{E}[\|\mathbf{w}_t - \mathbf{w}^*\|_2^2] - \lambda_t \frac{1}{2} \tau \mathbb{E}\left[F(\mathbf{w}_t) - F^*\right] + \lambda_t^2 \left(\frac{2\tau^3 + \tau}{3} G^2 + 4\tau L\Gamma + \frac{\tau^2 G^2 \sigma^2}{P_1} \mathbb{E}\left[\max_{k \in \mathcal{K}} \frac{\rho_k^2}{|h_k|^2}\right]\right).$$
 (58)

Next, we introduce the following lemma to bound the expected value of the training loss.

<u>Lemma</u> C.2: Suppose that two sequences $\{a_t : a_t \ge 0\}$ and $\{e_t : e_t \ge 0\}$ satisfy

$$a_{t+1} \le \left(1 - \frac{\mu \lambda_t \tau}{2}\right) a_t - \lambda_t e_t A + \lambda_t^2 C,\tag{59}$$

for $\lambda_t = \frac{8}{\mu\tau(\gamma+t)}$ and constants $A>0, C\geq 0, \mu>0, \gamma\geq 1$. Then, we have

$$\frac{A}{S_T} \sum_{t=0}^{T-1} \eta_t e_t \le \frac{\mu \gamma^3 \tau}{8S_T} a_0 + \frac{4T(T+2\gamma)}{\mu \tau S_T} C, \tag{60}$$

for $\eta_t = (\gamma + t)^2$ and $S_T \triangleq \sum_{t=0}^{T-1} \eta_t$.

Proof: The result in (60) follows from [25, Lemma 3.4].

By the convexity of $F(\cdot)$, we have

$$\mathbb{E}[F(\hat{\mathbf{w}}_T) - F^*] = \mathbb{E}\left[F\left(\frac{1}{S_T}\sum_{t=0}^{T-1}\eta_t\mathbf{w}_t\right) - F^*\right] \le \frac{1}{S_T}\sum_{t=0}^{T-1}\eta_t\mathbb{E}[F(\mathbf{w}_t) - F^*]. \tag{61}$$

The definitions of L and μ yield $\frac{L}{\mu} \geq 1$. Let $\gamma \geq \frac{16L}{\mu} \geq 1$ be a given constant. We note that $\lambda_t = \frac{8}{\mu\tau(\gamma+t)}$ satisfies the condition of Lemma C.1, i.e., $\lambda_t \leq \frac{1}{2L\tau}$. Therefore, substituting $a_t = \mathbb{E}[\|\mathbf{w}_t - \mathbf{w}^*\|_2^2]$, $e_t = \mathbb{E}\left[F(\mathbf{w}_t) - F^*\right]$, $A = \frac{1}{2}\tau$, and $C = \frac{2\tau^3 + \tau}{3}G^2 + 4\tau L\Gamma + \frac{\tau^2 G^2 \sigma^2}{P_1}\mathbb{E}\left[\max_{k \in \mathcal{K}} \frac{\rho_k^2}{|h_k|^2}\right]$ into (58), we obtain from Lemma C.2 and (61) that

$$\frac{1}{2}\tau \mathbb{E}[F(\hat{\mathbf{w}}_T) - F^*] \le \frac{4T(T + 2\gamma)}{\mu\tau S_T} \left(\frac{2\tau^3 + \tau}{3}G^2 + 4\tau L\Gamma + \frac{\tau^2 G^2 \sigma^2}{P_1} \mathbb{E}\left[\max_{k \in \mathcal{K}} \frac{\rho_k^2}{|h_k|^2}\right]\right) + \frac{\mu\gamma^3 \tau}{8S_T} \mathbb{E}[\|\mathbf{w}_0 - \mathbf{w}^*\|_2^2]. \tag{62}$$

Dividing both sides of (62) by $\frac{1}{2}\tau$, we have (24).

APPENDIX D

PROOF OF PROPOSITION 4.1

Since $\lim_{x\to\infty} F_{\hat{g}_{m,s}}(x) = 1$, we can compute the PDF of $\hat{g}_{m,s}$ as

$$f_{\hat{g}_{m,s}}(x) = \frac{f_{\bar{g}_{m,s}}(x) \cdot \mathbf{1}_{x \ge q}}{\int_{q}^{\infty} f_{\bar{g}_{m,s}}(x) dx} = \frac{f_{\bar{g}_{m,s}}(x) \cdot \mathbf{1}_{x \ge q}}{1 - F_{\bar{g}_{m,s}}(q)} = \begin{cases} \frac{Ne^{-x}(1 - e^{-x})^{N-1}}{p_{\text{IT}}}, & x \ge q. \\ 0, & \text{otherwise.} \end{cases}$$
(63)

Therefore, we have

$$\mathbb{E}\left[R_{\mathrm{avg}}\right] = p_{\mathrm{IT}} \mathbb{E}\left[\log_2\left(1 + \theta \hat{g}_{m,s}\right)\right] = p_{\mathrm{IT}} \int_{-\infty}^{\infty} \log_2\left(1 + \theta x\right) f_{\hat{g}_{m,s}}(x) dx$$

$$\stackrel{(a)}{=} \int_{q}^{\infty} \log_2(1+\theta x) N e^{-x} \sum_{i=0}^{N-1} \binom{N-1}{i} (-e^{-x})^i dx = N \sum_{i=0}^{N-1} \frac{\binom{N-1}{i}(-1)^i}{\ln 2} \int_{q}^{\infty} \ln(1+\theta x) e^{-(i+1)x} dx, \quad (64)$$

where (a) is from the binomial expansion. Moreover, we have the following integral formula [36, eq. (3.352.2), p. 340]

$$\int_{a}^{\infty} \ln(1+\vartheta)e^{-\omega\vartheta}d\vartheta = \ln(1+a)\frac{e^{-\omega a}}{\omega} + \frac{1}{\omega}\int_{a}^{\infty} \frac{e^{-\omega\vartheta}}{1+\vartheta}d\vartheta = \frac{1}{\omega}\left[\ln(1+a)e^{-\omega a} + e^{\omega}E_{1}(\omega a + \omega)\right]. \tag{65}$$

Substituting (65) into (64) with $\theta = \theta x$ and $\omega = \frac{i+1}{\theta}$, we obtain the result in (46).

APPENDIX E

PROOF OF PROPOSITION 4.2

From (40), we have

$$\mathbb{E}\big[\hat{R}_{\text{avg}}\big] = p_{\text{IT}} \mathbb{E}\left[\log_2(1 + \theta \bar{g}_{m,s})\right] = p_{\text{IT}} \int_{-\infty}^{\infty} \log_2(1 + \theta x) f_{\bar{g}_{m,s}}(x) dx$$

$$\stackrel{(a)}{=} p_{\text{IT}} \int_0^\infty \log_2\left(1 + \theta x\right) N e^{-x} \sum_{i=0}^{N-1} \binom{N-1}{i} (-e^{-x})^i dx = p_{\text{IT}} N \sum_{i=0}^{N-1} \frac{\binom{N-1}{i} (-1)^i}{(i+1) \ln 2} e^{\frac{i+1}{\theta}} E_1 \left(\frac{i+1}{\theta}\right), \quad (66)$$

where (a) is from the binomial expansion, and the last equality follows from (64) and (65) with $a=0,\ \theta=\theta x$ and $\omega=\frac{i+1}{\theta}$. Note that the condition $q=-\ln\left(1-\sqrt[N]{1-p_{\rm IT}}\right)$ is equivalent to

$$p_{\rm IT} = 1 - (1 - e^{-q})^N. (67)$$

Plugging (67) into (66), we have

$$\mathbb{E}\left[\hat{R}_{\text{avg}}\right] = N \sum_{i=0}^{N-1} \frac{\binom{N-1}{i}(-1)^{i}}{(i+1)\ln 2} \left[e^{\frac{i+1}{\theta}} E_{1} \left(\frac{i+1}{\theta}\right) - (1 - e^{-q})^{N} e^{\frac{i+1}{\theta}} E_{1} \left(\frac{i+1}{\theta}\right) \right]. \tag{68}$$

Note that $\varrho(q) \triangleq \mathbb{E}[R_{\text{avg}}] - \mathbb{E}[\hat{R}_{\text{avg}}]$. By (46) and (68), we have

$$\varrho(q) = N \sum_{i=0}^{N-1} \frac{\binom{N-1}{i}(-1)^i}{(i+1)\ln 2} \left[\ln(1+\theta q)e^{-(i+1)q} + e^{\frac{i+1}{\theta}} E_1 \left(\frac{i+1}{\theta} + (i+1)q \right) - e^{\frac{i+1}{\theta}} E_1 \left(\frac{i+1}{\theta} \right) \right]$$

$$+ (1 - e^{-q})^N e^{\frac{i+1}{\theta}} E_1 \left(\frac{i+1}{\theta} \right)$$
 (69)

Taking the derivative of $\varrho(q)$, we have

$$\varrho'(q) = N \sum_{i=0}^{N-1} \frac{\binom{N-1}{i}(-1)^{i}}{(i+1)\ln 2} N e^{-q} (1 - e^{-q})^{N-1} e^{\frac{i+1}{\theta}} E_{1} \left(\frac{i+1}{\theta}\right) - \frac{N \ln(1 + \theta q) e^{-q}}{\ln 2} \sum_{i=0}^{N-1} \binom{N-1}{i} (-e^{-q})^{i}$$

$$\stackrel{\underline{(b)}}{=} \frac{N e^{-q} (1 - e^{-q})^{N-1}}{\ln 2} \left[N \sum_{i=0}^{N-1} \frac{\binom{N-1}{i}(-1)^{i}}{i+1} e^{\frac{i+1}{\theta}} E_{1} \left(\frac{i+1}{\theta}\right) - \ln(1 + \theta q) \right]$$

$$\stackrel{\underline{(c)}}{=} \frac{N e^{-q} (1 - e^{-q})^{N-1}}{\ln 2} \left[\mathbb{E} \left[\ln \left(1 + \theta \bar{g}_{m,s} \right) \right] - \ln(1 + \theta q) \right], \tag{70}$$

where we have applied the property $E_1'(z) = -\frac{e^{-z}}{z}$, (b) is from the binomial expansion, and (c) is from (66).

Define $R \triangleq \mathbb{E} \left[\ln \left(1 + \theta \bar{q}_{m,s} \right) \right]$. By setting $\rho'(q^*) = 0$, we have

$$R - \ln(1 + \theta q^*) = 0 \quad \Rightarrow \quad q^* = \frac{e^R - 1}{\theta}.$$
 (71)

By (40), we have $\mathbb{E}[\bar{g}_{m,s}] > 0$. Since $\theta = \frac{P_2}{\phi \sigma^2} > 0$, R > 0 and thus $q^* > 0$. It follows from (70) that $\varrho'(q) > 0$ when $0 \le q < q^*$ and $\varrho'(q) < 0$ when $q > q^*$. Moreover, it is observed from (69) that $\varrho(0) = \lim_{q \to \infty} \varrho(q) = 0$. Therefore, we conclude that $\varrho(q) \ge 0$ for all q.

APPENDIX F

PROOF OF LEMMA C.1

Let $\mathbf{v}_{t+1} \in \mathbb{R}^{d \times 1}$ be the *virtual* global model vector obtained from model aggregation without communication error in the t-th communication round. That is, \mathbf{v}_{t+1} is given by

$$\mathbf{v}_{t+1} = \mathbf{w}_t + \mathbf{r}_t. \tag{72}$$

Then, we have

$$\mathbb{E}\left[\|\mathbf{w}_{t+1} - \mathbf{w}^*\|_2^2\right] = \mathbb{E}\left[\|\mathbf{w}_{t+1} - \mathbf{v}_{t+1}\|_2^2\right] + \mathbb{E}\left[\|\mathbf{v}_{t+1} - \mathbf{w}^*\|_2^2\right] + 2\mathbb{E}\left[\langle\mathbf{w}_{t+1} - \mathbf{v}_{t+1}, \mathbf{v}_{t+1} - \mathbf{w}^*\rangle\right]$$

$$= \mathbb{E}\left[\|\hat{\mathbf{r}}_t - \mathbf{r}_t\|_2^2\right] + \mathbb{E}\left[\|\mathbf{v}_{t+1} - \mathbf{w}^*\|_2^2\right] + 2\mathbb{E}\left[\langle\hat{\mathbf{r}}_t - \mathbf{r}_t, \mathbf{v}_{t+1} - \mathbf{w}^*\rangle\right],$$
(73)

where the last equality is because $\mathbf{w}_{t+1} - \mathbf{v}_{t+1} = \mathbf{w}_t + \hat{\mathbf{r}}_t - \mathbf{w}_t - \mathbf{r}_t = \hat{\mathbf{r}}_t - \mathbf{r}_t$.

Note that

$$\mathbb{E}\left[\hat{r}_{t}[i] - r_{t}[i]\right] = \mathbb{E}\left[\sum_{k=1}^{K} \left(\frac{c_{t}[i]h_{k,\Phi_{t}[i]}p_{k,\Phi_{t}[i]}}{\nu_{k,t}} - \rho_{k}\right) \left(\Delta_{k,t}[i] - \overline{\Delta}_{k,t}\right) + c_{t}[i]z_{t}[i]\right] = 0,\tag{74}$$

where the last equality is because $\mathbb{E}\left[z_t[i]\right] = 0$ and $\frac{c_t[i]h_{k,\Phi_t[i]}p_{k,\Phi_t[i]}}{\nu_{k,t}} - \rho_k = 0$, which is achieved by substituting the optimal $\{p_{k,\Phi_t[i]},c_t[i]\}$ given in (21). Consequently, we have $\mathbb{E}\left[\hat{\mathbf{r}}_t - \mathbf{r}_t\right] = 0$ and thus $\mathbb{E}\left[\langle \hat{\mathbf{r}}_t - \mathbf{r}_t, \mathbf{v}_{t+1} - \mathbf{w}^* \rangle\right] = 0$.

Since $\mathbf{v}_{t+1} = \mathbf{w}_t + \mathbf{r}_t$, we have

$$\mathbb{E}\left[\|\mathbf{v}_{t+1} - \mathbf{w}^*\|_2^2\right] = \mathbb{E}\left[\|\mathbf{w}_t - \mathbf{w}^*\|_2^2\right] + \mathbb{E}\left[\|\mathbf{r}_t\|_2^2\right] + 2\mathbb{E}\left[\langle \mathbf{w}_t - \mathbf{w}^*, \mathbf{r}_t \rangle\right]. \tag{75}$$

By the convexity of $\|\cdot\|_2^2$ and Assumption 3, we have

$$\mathbb{E}\left[\|\mathbf{r}_{t}\|_{2}^{2}\right] = \mathbb{E}\left[\left\|-\lambda_{t}\sum_{k=1}^{K}\rho_{k}\sum_{l=1}^{\tau}\nabla F_{k}(\mathbf{w}_{k,t}^{l},\xi_{k,t}^{l})\right\|_{2}^{2}\right] \leq \lambda_{t}^{2}\sum_{k=1}^{K}\rho_{k}\mathbb{E}\left[\left\|\sum_{l=1}^{\tau}\nabla F_{k}(\mathbf{w}_{k,t}^{l},\xi_{k,t}^{l})\right\|_{2}^{2}\right] \leq \lambda_{t}^{2}\tau^{2}G^{2}. \quad (76)$$

Moreover, we have

$$\mathbb{E}\left[\langle \mathbf{w}_{t} - \mathbf{w}^{*}, \mathbf{r}_{t} \rangle\right] = -\lambda_{t} \sum_{k=1}^{K} \rho_{k} \sum_{l=1}^{\tau} \mathbb{E}\left[\langle \mathbf{w}_{t} - \mathbf{w}^{*}, \nabla F_{k}(\mathbf{w}_{k,t}^{l}, \xi_{k,t}^{l}) \rangle\right]$$

$$= -\lambda_{t} \sum_{k=1}^{K} \rho_{k} \sum_{l=1}^{\tau} \mathbb{E}\left[\langle \mathbf{w}_{t} - \mathbf{w}_{k,t}^{l} + \mathbf{w}_{k,t}^{l} - \mathbf{w}^{*}, \nabla F_{k}(\mathbf{w}_{k,t}^{l}) \rangle\right]$$

$$= -\lambda_{t} \sum_{k=1}^{K} \rho_{k} \sum_{l=2}^{\tau} \mathbb{E}\left[\langle \mathbf{w}_{t} - \mathbf{w}_{k,t}^{l}, \nabla F_{k}(\mathbf{w}_{k,t}^{l}) \rangle\right] - \lambda_{t} \sum_{k=1}^{K} \rho_{k} \sum_{l=1}^{\tau} \mathbb{E}\left[\langle \mathbf{w}_{k,t}^{l} - \mathbf{w}^{*}, \nabla F_{k}(\mathbf{w}_{k,t}^{l}) \rangle\right], \quad (77)$$

where the second equality is because $\mathbb{E}[\nabla F_k(\mathbf{w}_{k,t}^l, \xi_{k,t}^l)] = \nabla F_k(\mathbf{w}_{k,t}^l)$ due to the uniform randomness of local stochastic gradients, and the last equality is from the fact that $\mathbf{w}_{k,t}^1 = \mathbf{w}_t$.

By the Cauchy-Schwarz inequality and the inequality of arithmetic and geometric means (AM-GM inequality), we have

$$-2\langle \mathbf{w}_t - \mathbf{w}_{k,t}^l, \nabla F_k(\mathbf{w}_{k,t}^l) \rangle \le \frac{1}{\lambda_t} \|\mathbf{w}_t - \mathbf{w}_{k,t}^l\|_2^2 + \lambda_t \|\nabla F_k(\mathbf{w}_{k,t}^l)\|_2^2.$$
(78)

By the μ -strong convexity of $F_k(\cdot)$, we have

$$-\langle \mathbf{w}_{k,t}^l - \mathbf{w}^*, \nabla F_k(\mathbf{w}_{k,t}^l) \rangle \le -\left(F_k(\mathbf{w}_{k,t}^l) - F_k(\mathbf{w}^*)\right) - \frac{\mu}{2} \|\mathbf{w}_{k,t}^l - \mathbf{w}^*\|_2^2. \tag{79}$$

By the L-smoothness of $F_k(\cdot)$, we have

$$\|\nabla F_k(\mathbf{w}_{k,t}^l)\|_2^2 \le 2L(F_k(\mathbf{w}_{k,t}^l) - F_k^*). \tag{80}$$

Since $\|a + b\|_2^2 \le 2\|a\|_2^2 + 2\|b\|_2^2$, we further have

$$-\|\mathbf{w}_{k,t}^{l} - \mathbf{w}^{*}\|_{2}^{2} \leq \|\mathbf{w}_{t} - \mathbf{w}_{k,t}^{l}\|_{2}^{2} - \frac{1}{2}\|\mathbf{w}_{t} - \mathbf{w}^{*}\|_{2}^{2}.$$
(81)

Combining (75)-(81), we obtain

$$\mathbb{E}\left[\|\mathbf{v}_{t+1} - \mathbf{w}^*\|_{2}^{2}\right] \leq \mathbb{E}\left[\|\mathbf{w}_{t} - \mathbf{w}^*\|_{2}^{2}\right] + \lambda_{t}^{2}\tau^{2}G^{2} + \lambda_{t}\sum_{k=1}^{K}\rho_{k}\sum_{l=2}^{\tau}\mathbb{E}\left[\frac{1}{\lambda_{t}}\|\mathbf{w}_{t} - \mathbf{w}_{k,t}^{l}\|_{2}^{2} + \lambda_{t}\|\nabla F_{k}(\mathbf{w}_{k,t}^{l})\|_{2}^{2}\right] \\
- 2\lambda_{t}\sum_{k=1}^{K}\rho_{k}\sum_{l=1}^{\tau}\mathbb{E}\left[F_{k}(\mathbf{w}_{k,t}^{l}) - F_{k}(\mathbf{w}^*) + \frac{\mu}{2}\|\mathbf{w}_{k,t}^{l} - \mathbf{w}^*\|_{2}^{2}\right] \\
\leq \mathbb{E}\left[\|\mathbf{w}_{t} - \mathbf{w}^*\|_{2}^{2}\right] + \lambda_{t}^{2}\tau^{2}G^{2} + \lambda_{t}^{2}\sum_{k=1}^{K}\rho_{k}\sum_{l=2}^{\tau}\mathbb{E}\left[2L(F_{k}(\mathbf{w}_{k,t}^{l}) - F_{k}^{*})\right] \\
+ \sum_{k=1}^{K}\rho_{k}\sum_{l=2}^{\tau}\mathbb{E}\left[\|\mathbf{w}_{t} - \mathbf{w}_{k,t}^{l}\|_{2}^{2}\right] - 2\lambda_{t}\sum_{k=1}^{K}\rho_{k}\sum_{l=1}^{\tau}\mathbb{E}\left[F_{k}(\mathbf{w}_{k,t}^{l}) - F_{k}(\mathbf{w}^{*})\right] \\
+ \mu\lambda_{t}\sum_{k=1}^{K}\rho_{k}\sum_{l=1}^{\tau}\left(\mathbb{E}\left[\|\mathbf{w}_{t} - \mathbf{w}_{k,t}^{l}\|_{2}^{2}\right] - \frac{1}{2}\mathbb{E}\left[\|\mathbf{w}_{t} - \mathbf{w}^{*}\|_{2}^{2}\right]\right) \\
\leq \left(1 - \frac{\mu\lambda_{t}\tau}{2}\right)\mathbb{E}\left[\|\mathbf{w}_{t} - \mathbf{w}^{*}\|_{2}^{2}\right] + \lambda_{t}^{2}\tau^{2}G^{2} + (1 + \mu\lambda_{t})\sum_{k=1}^{K}\rho_{k}\sum_{l=2}^{\tau}\mathbb{E}\left[\|\mathbf{w}_{k,t}^{l} - \mathbf{w}_{t}\|_{2}^{2}\right] \\
+ 2L\lambda_{t}^{2}\sum_{k=1}^{K}\rho_{k}\sum_{l=1}^{\tau}\mathbb{E}\left[F_{k}(\mathbf{w}_{k,t}^{l}) - F_{k}^{*}\right] - 2\lambda_{t}\sum_{k=1}^{K}\rho_{k}\sum_{l=1}^{\tau}\mathbb{E}\left[F_{k}(\mathbf{w}_{k,t}^{l}) - F_{k}(\mathbf{w}^{*})\right], \quad (82)$$

where (a) is from (80) and (81), and (b) is from the facts that $\mathbf{w}_{k,t}^1 = \mathbf{w}_t$ and $\sum_{k=1}^K \rho_k = 1$. Define $\psi_t = 2\lambda_t(1 - L\lambda_t)$. Since $\lambda_t \leq \frac{1}{2L\tau}$ and $\tau \geq 1$, we have $1 - L\lambda_t \geq 1 - \frac{1}{2\tau} \geq \frac{1}{2}$ and thus $\lambda_t \leq \psi_t \leq 2\lambda_t$. Then, we have:

$$2L\lambda_{t}^{2} \sum_{k=1}^{K} \rho_{k} \sum_{l=1}^{\tau} \mathbb{E}\left[F_{k}(\mathbf{w}_{k,t}^{l}) - F_{k}^{*}\right] - 2\lambda_{t} \sum_{k=1}^{K} \rho_{k} \sum_{l=1}^{\tau} \mathbb{E}\left[F_{k}(\mathbf{w}_{k,t}^{l}) - F_{k}(\mathbf{w}^{*})\right]$$

$$= -2\lambda_{t}(1 - L\lambda_{t}) \sum_{k=1}^{K} \rho_{k} \sum_{l=1}^{\tau} \mathbb{E}\left[F_{k}(\mathbf{w}_{k,t}^{l}) - F_{k}^{*}\right] + 2\lambda_{t} \sum_{k=1}^{K} \rho_{k} \sum_{l=1}^{\tau} \mathbb{E}\left[F_{k}(\mathbf{w}^{*}) - F_{k}^{*}\right]$$

$$= -\psi_{t} \sum_{k=1}^{K} \rho_{k} \sum_{l=1}^{\tau} \mathbb{E}\left[F_{k}(\mathbf{w}_{k,t}^{l}) - F_{k}(\mathbf{w}^{*}) + F_{k}(\mathbf{w}^{*}) - F_{k}^{*}\right] + 2\lambda_{t} \sum_{k=1}^{K} \rho_{k} \sum_{l=1}^{\tau} \mathbb{E}\left[F_{k}(\mathbf{w}^{*}) - F_{k}^{*}\right]$$

$$\stackrel{(c)}{=} -\psi_{t} \sum_{k=1}^{K} \rho_{k} \sum_{l=1}^{\tau} \mathbb{E}\left[F_{k}(\mathbf{w}_{k,t}^{l}) - F^{*}\right] + (2\lambda_{t} - \psi_{t}) \sum_{l=1}^{\tau} \left(F^{*} - \sum_{k=1}^{K} \rho_{k} F_{k}^{*}\right)$$

$$\stackrel{(d)}{=} -\psi_{t} \sum_{k=1}^{K} \rho_{k} \sum_{l=1}^{\tau} \mathbb{E}\left[F_{k}(\mathbf{w}_{k,t}^{l}) - F^{*}\right] + 2\lambda_{t}^{2} \tau L\Gamma, \tag{83}$$

where (c) is because $\sum_{k=1}^{K} \rho_k F^* = F^* = \sum_{k=1}^{K} \rho F_k(\mathbf{w}^*)$, and (d) is because $\Gamma = \sum_{k=1}^{K} \rho_k (F^* - F_k^*) = F^* - \sum_{k=1}^{K} \rho_k F_k^*$.

To bound the first term on the r.h.s. of (83), we have

$$\sum_{k=1}^{K} \rho_{k} \sum_{l=1}^{\tau} \mathbb{E}\left[F_{k}(\mathbf{w}_{k,t}^{l}) - F^{*}\right] = \sum_{k=1}^{K} \rho_{k} \sum_{l=1}^{\tau} \mathbb{E}\left[F_{k}(\mathbf{w}_{k,t}^{l}) - F_{k}(\mathbf{w}_{t}) + F_{k}(\mathbf{w}_{t}) - F^{*}\right]$$

$$\stackrel{(e)}{\geq} \sum_{k=1}^{K} \rho_{k} \sum_{l=1}^{\tau} \mathbb{E}\left[\langle \nabla F_{k}(\mathbf{w}_{t}), \mathbf{w}_{k,t}^{l} - \mathbf{w}_{t} \rangle + \frac{\mu}{2} \|\mathbf{w}_{k,t}^{l} - \mathbf{w}_{t}\|_{2}^{2}\right] + \tau \mathbb{E}\left[F(\mathbf{w}_{t}) - F^{*}\right]$$

$$\stackrel{(f)}{\geq} \sum_{k=1}^{K} \rho_{k} \sum_{l=1}^{\tau} \mathbb{E}\left[-\frac{\lambda_{t}}{2} \|\nabla F_{k}(\mathbf{w}_{t})\|_{2}^{2} - \frac{1}{2\lambda_{t}} \|\mathbf{w}_{k,t}^{l} - \mathbf{w}_{t}\|_{2}^{2}\right]$$

$$+ \frac{\mu}{2} \sum_{k=1}^{K} \rho_{k} \sum_{l=1}^{\tau} \mathbb{E}\left[\|\mathbf{w}_{k,t}^{l} - \mathbf{w}_{t}\|_{2}^{2}\right] + \tau \mathbb{E}\left[F(\mathbf{w}_{t}) - F^{*}\right]$$

$$\stackrel{(g)}{\geq} - \sum_{k=1}^{K} \rho_{k} \sum_{l=1}^{\tau} \mathbb{E}\left[\lambda_{t} L(F_{k}(\mathbf{w}_{t}) - F_{k}^{*})\right] + \tau \mathbb{E}\left[F(\mathbf{w}_{t}) - F^{*}\right]$$

$$- \left(\frac{1}{2\lambda_{t}} - \frac{\mu}{2}\right) \sum_{k=1}^{K} \rho_{k} \sum_{l=1}^{\tau} \mathbb{E}\left[\|\mathbf{w}_{k,t}^{l} - \mathbf{w}_{t}\|_{2}^{2}\right], \tag{84}$$

where (e) is from the μ -strong convexity of $F_k(\cdot)$, (f) is from the AM-GM inequality and (g) is from (80). Substituting (84) into (83), we have

$$2L\lambda_{t}^{2}\sum_{k=1}^{K}\rho_{k}\sum_{l=1}^{\gamma}\mathbb{E}\left[F_{k}(\mathbf{w}_{k,t}^{l})-F_{k}^{*}\right]-2\lambda_{t}\sum_{k=1}^{K}\rho_{k}\sum_{l=1}^{\gamma}\mathbb{E}\left[F_{k}(\mathbf{w}_{k,t}^{l})-F_{k}(\mathbf{w}^{*})\right]$$

$$\leq\psi_{t}\sum_{k=1}^{K}\rho_{k}\sum_{l=1}^{\tau}\mathbb{E}\left[\lambda_{t}L(F_{k}(\mathbf{w}_{t})-F^{*}+F^{*}-F_{k}^{*})\right]+\psi_{t}\left(\frac{1}{2\lambda_{t}}-\frac{\mu}{2}\right)\sum_{k=1}^{K}\rho_{k}\sum_{l=1}^{\tau}\mathbb{E}\left[\|\mathbf{w}_{k,t}^{l}-\mathbf{w}_{t}\|_{2}^{2}\right]$$

$$-\psi_{t}\tau\mathbb{E}\left[F(\mathbf{w}_{t})-F^{*}\right]+2\lambda_{t}^{2}\tau L\Gamma$$

$$=\psi_{t}(\lambda_{t}L-1)\tau\sum_{k=1}^{K}\rho_{k}\mathbb{E}\left[F_{k}(\mathbf{w}_{t})-F^{*}\right]+\psi_{t}\left(\frac{1}{2\lambda_{t}}-\frac{\mu}{2}\right)\sum_{k=1}^{K}\rho_{k}\sum_{l=1}^{\tau}\mathbb{E}\left[\|\mathbf{w}_{k,t}^{l}-\mathbf{w}_{t}\|_{2}^{2}\right]+\left(2\lambda_{t}^{2}\tau+\psi_{t}\lambda_{t}\tau\right)L\Gamma$$

$$\stackrel{(h)}{\leq}-\frac{1}{2}\lambda_{t}\tau\mathbb{E}\left[F(\mathbf{w}_{t})-F^{*}\right]+(1-\mu\lambda_{t})\sum_{k=1}^{K}\rho_{k}\sum_{l=2}^{\tau}\mathbb{E}\left[\|\mathbf{w}_{k,t}^{l}-\mathbf{w}_{t}\|_{2}^{2}\right]+4\lambda_{t}^{2}\tau L\Gamma,$$

$$(85)$$

where (h) is due to the following facts, with each corresponding to one term:

1)
$$\lambda_t L - 1 \le \frac{1}{2\tau} - 1 \le -\frac{1}{2}$$
, $\lambda_t \le \psi_t \le 2\lambda_t$, and $\sum_{k=1}^K \rho_k(F_k(\mathbf{w}_t) - F^*) = F(\mathbf{w}_t) - F^* \ge 0$;

2)
$$L \ge \mu$$
, $\frac{1}{2\lambda_t} - \frac{\mu}{2} \ge L\tau - \frac{\mu}{2} \ge 0$, $\psi_t(\frac{1}{2\lambda_t} - \frac{\mu}{2}) \le 2\lambda_t(\frac{1}{2\lambda_t} - \frac{\mu}{2}) = (1 - \mu\lambda_t)$, and $\mathbf{w}_{k,t}^1 = \mathbf{w}_t$;

3)
$$\Gamma \geq 0$$
 and $2\lambda_t^2 \tau + \psi_t \lambda_t \tau \leq 4\lambda_t^2 \tau$.

Substituting (85) into (82), we have

$$\mathbb{E}\left[\|\mathbf{v}_{t+1} - \mathbf{w}^*\|_2^2\right] \le \left(1 - \frac{\mu \lambda_t \tau}{2}\right) \mathbb{E}\left[\|\mathbf{w}_t - \mathbf{w}^*\|_2^2\right] - \frac{1}{2}\lambda_t \tau \mathbb{E}\left[F(\mathbf{w}_t) - F^*\right] + \lambda_t^2 \tau^2 G^2$$

$$+ 2\sum_{k=1}^K \rho_k \sum_{l=2}^{\tau} \mathbb{E}\left[\|\mathbf{w}_{k,t}^l - \mathbf{w}_t\|_2^2\right] + 4\lambda_t^2 \tau L\Gamma. \tag{86}$$

Plugging (86) and $\mathbb{E}\left[\langle \hat{\mathbf{r}}_t - \mathbf{r}_t, \mathbf{v}_{t+1} - \mathbf{w}^* \rangle\right] = 0$ into (73) gives the result in (55).

REFERENCES

- [1] Z. Zhou, X. Chen, E. Li, L. Zeng, K. Luo, and J. Zhang, "Edge intelligence: Paving the last mile of artificial intelligence with edge computing," *Proc. IEEE*, vol. 107, no. 8, pp. 1738–1762, Aug. 2019.
- [2] J. Park, S. Samarakoon, M. Bennis, and M. Debbah, "Wireless network intelligence at the edge," *Proc. IEEE*, vol. 107, no. 11, pp. 2204–2239, Nov. 2019.
- [3] K. B. Letaief, W. Chen, Y. Shi, J. Zhang, and Y.-J. A. Zhang, "The roadmap to 6G: AI empowered wireless networks," *IEEE Commun. Mag.*, vol. 57, no. 8, pp. 84–90, Aug. 2019.
- [4] B. McMahan, E. Moore, D. Ramage, S. Hampson, and B. A. Y. Arcas, "Communication-efficient learning of deep networks from decentralized data," in *Proc. Int. Conf. Artif. Intell. Statist. (AISTATS)*, vol. 54, Apr. 2017, pp. 1273–1282.
- [5] B. Nazer and M. Gastpar, "Computation over multiple-access channels," *IEEE Trans. Inf. Theory*, vol. 53, no. 10, pp. 3498–3516, Oct. 2007.
- [6] K. Yang, T. Jiang, Y. Shi, and Z. Ding, "Federated learning via over-the-air computation," *IEEE Trans. Wireless Commun.*, vol. 19, no. 3, pp. 2022–2035, Mar. 2020.
- [7] H. Liu, X. Yuan, and Y.-J. A. Zhang, "Reconfigurable intelligent surface enabled federated learning: A unified communication-learning design approach," *IEEE Trans. Wireless Commun.*, vol. 20, no. 11, pp. 7595–7609, Nov. 2021.
- [8] Z. Lin, H. Liu, and Y.-J. A. Zhang, "Relay-assisted over-the-air federated learning," in *Proc. IEEE Globecom Workshops* (*GC Wkshps*), Dec. 2021, pp. 1–7.
- [9] X. Cao, G. Zhu, J. Xu, Z. Wang, and S. Cui, "Optimized power control design for over-the-air federated edge learning," *IEEE J. Sel. Areas Commun.*, vol. 40, no. 1, pp. 342–358, Jan. 2022.
- [10] N. Zhang and M. Tao, "Gradient statistics aware power control for over-the-air federated learning," *IEEE Trans. on Wireless Commun.*, vol. 20, no. 8, pp. 5115–5128, Aug. 2021.
- [11] C. Xu, S. Liu, Z. Yang, Y. Huang, and K.-K. Wong, "Learning rate optimization for federated learning exploiting over-the-air computation," *IEEE J. Sel. Areas Commun.*, vol. 39, no. 12, pp. 3742–3756, Dec. 2021.
- [12] D. Liu and O. Simeone, "Privacy for free: Wireless federated learning via uncoded transmission with adaptive power control," *IEEE J. Sel. Areas Commun.*, vol. 39, no. 1, pp. 170–185, Jan. 2021.
- [13] G. Zhu, Y. Wang, and K. Huang, "Broadband analog aggregation for low-latency federated edge learning," *IEEE Trans. Wireless Commun.*, vol. 19, no. 1, pp. 491–506, Jan. 2020.
- [14] W. Saad, M. Bennis, and M. Chen, "A vision of 6G wireless systems: Applications, trends, technologies, and open research problems," *IEEE Netw.*, vol. 34, no. 3, pp. 134–142, May 2019.

- [15] H. Tataria, M. Shafi, A. F. Molisch, M. Dohler, H. Sjöland, and F. Tufvesson, "6G wireless systems: Vision, requirements, challenges, insights, and opportunities," *Proc. IEEE*, vol. 109, no. 7, pp. 1166–1199, Jul. 2021.
- [16] K. B. Letaief, Y. Shi, J. Lu, and J. Lu, "Edge artificial intelligence for 6G: Vision, enabling technologies, and applications," *IEEE J. Sel. Areas Commun.*, vol. 40, no. 1, pp. 5–36, Jan. 2022.
- [17] Y. Lin, S. Han, H. Mao, Y. Wang, and W. J. Dally, "Deep gradient compression: Reducing the communication bandwidth for distributed training," in *Proc. Int. Conf. Learn. Represent. (ICLR)*, 2018.
- [18] D. Alistarh, D. Grubic, J. Li, R. Tomioka, and M. Vojnovic, "QSGD: Communication-efficient SGD via randomized quantization and encoding," in *Proc. Adv. Neural Inf. Process. Syst. (NIPS)*, vol. 3, Dec. 2017, pp. 1710–1721.
- [19] S. U. Stich, J.-B. Cordonnier, and M. Jaggi, "Sparsified SGD with memory," arXiv preprint arXiv:1809.07599, 2018.
- [20] J. Bernstein, Y.-X. Wang, K. Azizzadenesheli, and A. Anandkumar, "signSGD: Compressed optimisation for non-convex problems," in *Proc. Int. Conf. Mach. Learn. (ICML)*, 2018, pp. 560–569.
- [21] G. Zhu, Y. Du, D. Gündüz, and K. Huang, "One-bit over-the-air aggregation for communication-efficient federated edge learning: Design and convergence analysis," *IEEE Trans. Wireless Commun.*, vol. 20, no. 3, pp. 2120–2135, Mar. 2021.
- [22] M. M. Amiri and D. Gündüz, "Machine learning at the wireless edge: Distributed stochastic gradient descent over-the-air," *IEEE Trans. Signal Process.*, vol. 68, pp. 2155–2169, Mar. 2020.
- [23] —, "Federated learning over wireless fading channels," *IEEE Trans. Wireless Commun.*, vol. 19, no. 5, pp. 3546–3557, May 2020.
- [24] D. Fan, X. Yuan, and Y.-J. A. Zhang, "Temporal-structure-assisted gradient aggregation for over-the-air federated edge learning," *IEEE J. Sel. Areas Commun.*, vol. 39, no. 12, pp. 3757–3771, Dec. 2021.
- [25] S. U. Stich, "Local SGD converges fast and communicates little," in Proc. Int. Conf. Learn. Represent. (ICLR), 2019.
- [26] T. Li, A. K. Sahu, M. Zaheer, M. Sanjabi, A. Talwalkar, and V. Smith, "Federated optimization in heterogeneous networks," in *Proc. Mach. Learn. Syst. (MLSys)*, vol. 2, 2020, pp. 429–450.
- [27] X. Li, K. Huang, W. Yang, S. Wang, and Z. Zhang, "On the convergence of fedavg on non-iid data," in *Proc. Int. Conf. Learn. Represent. (ICLR)*, 2020.
- [28] S. Wang, T. Tuor, T. Salonidis, K. K. Leung, C. Makaya, T. He, and K. Chan, "Adaptive federated learning in resource constrained edge computing systems," *IEEE J. Sel. Areas Commun.*, vol. 37, no. 6, pp. 1205–1221, Jun. 2019.
- [29] M. M. Amiri, D. Gündüz, S. R. Kulkarni, and H. V. Poor, "Convergence of update aware device scheduling for federated learning at the wireless edge," *IEEE Trans. Wireless Commun.*, vol. 20, no. 6, pp. 3643–3658, Jun. 2021.
- [30] A. Krizhevsky, I. Sutskever, and G. E. Hinton, "Imagenet classification with deep convolutional neural networks," in *Proc. Adv. Neural Inf. Process. Syst. (NIPS)*, vol. 25, 2012.
- [31] J. Konečný, H. B. McMahan, D. Ramage, and P. Richtárik, "Federated optimization: Distributed machine learning for on-device intelligence," arXiv preprint arXiv:1610.02527, 2016. [Online]. Available: http://arxiv.org/abs/1610.02527
- [32] W. Shi, S. Zhou, Z. Niu, M. Jiang, and L. Geng, "Joint device scheduling and resource allocation for latency constrained wireless federated learning," *IEEE Trans. Wireless Commun.*, vol. 20, no. 1, pp. 453–467, Jan. 2021.
- [33] D. Soudry, D. Di Castro, A. Gal, A. Kolodny, and S. Kvatinsky, "Memristor-based multilayer neural networks with online gradient descent training," *IEEE Trans. Neural Netw. Learn. Syst.*, vol. 26, no. 10, pp. 2408–2421, Oct. 2015.
- [34] R. Pascanu, T. Mikolov, and Y. Bengio, "On the difficulty of training recurrent neural networks," in *Proc. Int. Conf. Mach. Learn. (ICML)*, Jun. 2013, pp. 1310–1318.
- [35] Z. Lin, H. Liu, and Y.-J. A. Zhang, "Relay-assisted cooperative federated learning," *IEEE Trans. Wireless Commun.*, Mar. 2022.
- [36] I. S. Gradshteyn and I. M. Ryzhik, Table of integrals, series, and products, 7th ed. Elsevier, 2007.